

1   **Moisture damage assessment using surface energy, bitumen stripping**  
2                   **and the SATS moisture conditioning procedure**

4                   James Grenfell, Alex Apeagyei and Gordon Airey

6                   Nottingham Transportation Engineering Centre, University of Nottingham,  
7                   Nottingham NG7 2RD, United Kingdom.

8                   Telephone: +44 115 9513905, Fax: +44 115 9513909

9                   Email: [james.grenfell@nottingham.ac.uk](mailto:james.grenfell@nottingham.ac.uk)

10

11   **Abstract**

12

13   Durability is one of the most important properties of an asphalt mixture. A key factor  
14   affecting the durability of asphalt pavements is moisture damage. Moisture damage  
15   generally results in the loss of strength of the mixture due to two main mechanisms;  
16   the loss of adhesion between bitumen and aggregate and the loss of cohesion within  
17   the mixture. Conventional test methods for evaluating moisture damage include tests  
18   conducted on loose bitumen-coated aggregates and those conducted on compacted  
19   asphalt mixtures. The former test methods are simpler and less expensive to conduct  
20   but are qualitative/subjective in nature and do not consider cohesive failure while the  
21   latter, though more quantitative, are based on bulky mechanical test set-ups and  
22   therefore require expensive equipment. Both test methods are, however, empirical in  
23   nature thus requiring extensive experience to interpret/use their results. The rolling  
24   bottle test (EN 12697-11) for loose aggregate mixtures and the Saturation Ageing  
25   Tensile Stiffness (SATS) test (EN 12697-45) for compacted asphalt mixtures are two  
26   such methods, which experience suggests, could clearly discriminate between ‘good’  
27   and ‘poor’ performing mixtures in the laboratory. A more fundamental approach  
28   based on surface energy (SE) measurements offers promise to better understand  
29   moisture damage. This paper looks at results from the rolling bottle and the SATS  
30   tests in an attempt to better understand the underlying processes and mechanisms of  
31   moisture damage with the help of surface energy measurements on the constituent  
32   bitumen and aggregates. For this work, a set of bitumens and typical acidic and basic  
33   aggregate types (granite and limestone) were selected. Combinations of these

34 materials were assessed using both the rolling bottle and SATS tests. The surface  
35 energy properties of the binders were measured using a Dynamic Contact Angle  
36 (DCA) Analyser and those of the aggregates using a Dynamic Vapour Sorption  
37 (DVS) device. From these surface energy measurements it was possible to predict the  
38 relative performance of both the simple rolling bottle test and the more complicated  
39 SATS test. Mineralogical composition of the aggregates determined using a Mineral  
40 Liberation Analyser (MLA) was used to explain the differences in performance of the  
41 mixtures considered.

42

43 Keywords: Bitumen; Asphalt mixtures; Surface energy; Moisture damage; SATS;  
44 Rolling Bottle Test, Adhesion, Mineralogical composition.

45

46

47

48

49

50

51

52

53

54

55

56

57

58

59

60

61

62

63

64

65

66

67

68     **1. Introduction**

69

70     The road network is one of the most important elements of a modern transportation  
71     system with the majority of roads throughout the world being constructed from  
72     asphalt mixtures. Across the United Kingdom, the total budget spent on road  
73     maintenance during 2009/10 was of the order of £3.8 billion with moisture damage  
74     considered to be one of the major causes of distress in asphalt pavements (Alarm,  
75     2010; Audit Scotland, 2010). Although not all damage is caused directly by moisture,  
76     its presence increases the extent and severity of already existing distresses like  
77     cracking, potholes and rutting (Kennedy et al., 1983; Miller and Bellinger, 2003). The  
78     presence of moisture results in the degradation of the mechanical properties of the  
79     asphalt mixture, i.e. loss of stiffness and mechanical strength, which ultimately leads  
80     to the failure of the road structure. Moisture damage thus has a great economic impact  
81     as it causes premature pavement failure and hence results in increased rehabilitation  
82     activities and maintenance costs.

83

84     The physical and chemical properties of the two main constituents of an asphalt  
85     mixture (bitumen and aggregate) have a direct influence on the moisture performance  
86     of the mixture. A lack of compatibility between bitumen and aggregate is one of the  
87     main reasons for distress with moisture damage normally being related to the loss of  
88     adhesion between bitumen and aggregate and/or loss of cohesion within the bitumen  
89     (or more realistically the bitumen-filler mastic) in the presence of water (Terrel and  
90     Al-Swailmi, 1994). Removal of bitumen film from the aggregate surface by water is  
91     known as ‘stripping’ with this phenomenon depending largely on the chemical  
92     composition of the bitumen and aggregates, and their affinity towards each other  
93     (Kandhal, 1994; Emery and Seddik, 1997). Previous studies have indicated that the  
94     susceptibility of asphalt mixtures to moisture attack is related to bitumen chemistry,  
95     aggregate mineralogy, surface texture of the aggregate and the adhesion between the  
96     bitumen and aggregates (Airey et al., 2008; Abo-Qudais and Al-Shweily, 2007;  
97     Hognies et al., 2011; Petersen et al., 1982). In addition, the ambient conditions  
98     (including temperature, freeze–thaw cycles and wetting–drying cycles) can also  
99     significantly affect the durability of an asphalt pavement material (Huang et al., 2005;  
100     Gilmore et al., 1985).

101

102 Numerous laboratory test methods have been developed over the years to determine  
103 the moisture susceptibility of asphalt mixtures and their response to moisture ingress  
104 (Airey and Choi, 2002; Solaimanian et al., 2003). These methods can be divided into  
105 two groups: (i) qualitative tests conducted on loose bitumen-coated aggregate, such as  
106 the boiling test (Kennedy et al., 1984), and (ii) quantitative tests conducted on  
107 compacted asphalt mixtures, such as the wheel tracking test (Aschenbrener, 1995) and  
108 the Saturation Ageing Tensile Stiffness (SATS) test procedure (Collop et al., 2004a;  
109 Collop et al., 2004a; Airey et al., 2005). The relevant test specimens are typically  
110 conditioned in water to simulate in-service conditions and an assessment of any  
111 moisture induced damage is made by dividing the conditioned modulus or strength by  
112 the corresponding unconditioned property, for example as in the freeze-thaw  
113 AASHTO T283-99 procedure (Anon, 2000). In addition to these laboratory test  
114 methods, a number of computational approaches have been developed to simulate the  
115 in-service conditions experienced by asphalt pavement materials, and hence to attempt  
116 to predict the durability and moisture resistance of such materials (Caro et al., 2008a;  
117 Caro et al., 2008b; Caro et al., 2010; Masad et al., 2007; Kutay et al., 2007; Shakiba et  
118 al., 2013).

119

120 Although these various approaches are realistic and logical in terms of simulating in-  
121 service asphalt pavement materials, they do not necessarily attempt to understand in  
122 detail the adhesion between bitumen and aggregates, and how such interactions are  
123 affected by the presence of moisture and other external factors. It is these physico-  
124 chemical properties, directly related to the adhesion characteristics of the two  
125 materials, that are responsible for adhesion or debonding between the materials (MS-  
126 24, 2007; Kennedy et al., 1982). Surface energy (or more correctly surface free energy  
127 (SFE)) properties of the materials can be used to assess these adhesion characteristics  
128 (Bhasin, 2006). SFE and various thermodynamic calculations can therefore be  
129 successfully used to assess the cohesive and adhesive bond strengths of the two  
130 materials and the effect of moisture/water on the bond strength of a bitumen-  
131 aggregate system (Bhasin et al., 2006; Cheng et al., 2002a; Cheng et al., 2002b). SFE  
132 can therefore be considered to truly represent the physico-chemical surface  
133 characteristics of bitumen and aggregates and has been successfully used as a tool for  
134 selection of moisture resistant materials (Cheng, 2002). The physico-chemical  
135 characteristics of bitumen and aggregates, which can be assessed using surface energy

136 principles, are believed to be a key factor responsible for the adhesion between the  
137 two materials.

138

139 This paper presents a framework of surface energy testing techniques with bitumen-  
140 aggregate stripping and asphalt mixture mechanical moisture sensitivity assessment  
141 for identification of compatible bitumen-aggregate combinations. A complete  
142 characterisation is possible once results from SFE measurements and intrinsic  
143 adhesion calculations are compared with those of standard mechanical moisture  
144 damage tests. Tests like the rolling bottle test (RBT) and the saturated ageing tensile  
145 stiffness (SATS) test have been used together with intrinsic adhesion and energy  
146 ratios to determine if the moisture sensitivity assessment parameters for different  
147 bitumen-aggregate combinations can identify ‘good’ and ‘poor’ performing asphalt  
148 mixtures and to determine how the surface energy-based predictions compare with  
149 conventional moisture damage test methods.

150

## 151 2. Intrinsic adhesion

152

### 153 2.1 Surface free energy theory

154

155 The surface free energy (SFE) of a material is defined as the energy needed to create a  
156 new unit surface area of the material in a vacuum condition. The surface energies of  
157 bitumen and aggregate or a bitumen-aggregate system (asphalt mixture) are mainly  
158 comprised of an apolar (nonpolar) component and an acid-base component (Fowkes,  
159 1962; Good and van Oss, 1991 and Good, 1992). Equation 1 is used to describe the  
160 total surface energy and its components:

161

$$162 \gamma = \gamma^{LW} + \gamma^{AB} \quad (1)$$

163

164 Where:  $\gamma$  = surface energy of bitumen or aggregate ( $\text{mJ/m}^2$ );

165  $\gamma^{LW}$  = Lifshitz–van der Waals component of the surface energy ( $\text{mJ/m}^2$ ); and

166  $\gamma^{AB}$  = acid-base component of the surface energy ( $\text{mJ/m}^2$ ).

167

168 The Lifshitz-van der Waals force contains at least three components: London  
169 dispersion forces, Debye induction forces, and Keesom orientation forces (Maugis,  
170 1999). The acid-base interaction includes all interactions of electron donor (proton  
171 acceptor) - electron acceptor (proton donor) type bonds including hydrogen bonding.  
172 To quantitatively predict and treat the acid-base interaction, Good and van Oss (1991)  
173 postulated a resolution of the acid-base term,  $\gamma^{AB}$  into a Lewis acidic surface  
174 parameter and a Lewis basic surface parameter. The relationship among the  $\gamma^{AB}$  and  
175 its components is shown in equation 2:

176

177 
$$\gamma^{AB} = 2\sqrt{\gamma^+ \gamma^-} \quad (2)$$

178

179 Where:  $\gamma^+$  = Lewis acid component of surface interaction, and

180  $\gamma^-$  = Lewis base component of surface interaction.

181

182 **2.2 SFE measurements**

183

184 Five bitumens were included in the study consisting of four conventional bitumens  
185 and one modified bitumen. The conventional bitumens ranged from very hard  
186 consistency (10/20 penetration grade) to very soft (160/220 pen grade) with  
187 intermediate grades of 40/60 pen and 70/100 pen. The modified bitumen was  
188 produced by mixing the 40/60 pen bitumen with an amine-based anti-stripping agent  
189 at 0.5% additive by weight of binder. Surface energy components of the five bitumens  
190 used in this study were determined indirectly using contact angle measurements.

191

192 A Cahn Model dynamic contact angle (DCA) analyser was used to measure the  
193 contact angles of a set of three carefully selected probe liquids on bitumen coated  
194 glass slides under dynamic conditions. The probe liquids used included water,  
195 glycerol and diiodomethane. All the tests were conducted at room temperature ( $23^\circ\text{C}$   
196  $\pm 2^\circ\text{C}$ ) and  $50\% \pm 5\%$  relative humidity.

197

198 During the test, a clean 40 mm x 24 mm x 0.45 mm No. 15 microscope glass slide  
199 was coated with bitumen and hung from the balance of the DCA equipment with the  
200 help of a crocodile clip. A beaker containing a probe liquid was placed on a movable

201 stage positioned under the glass slide. The bottom edge of the slide was kept parallel  
202 with the surface of the probe liquid. The bitumen-coated glass slide was then  
203 immersed up to a maximum depth of 5 mm (advancing) and then withdrawn  
204 (receding) from the liquid by moving the stage up and down, respectively, at a  
205 constant speed of 40 microns/sec while continuously recording the change in mass of  
206 the bitumen-coated slide with depth of immersion. The measured mass-depth  
207 relationships were used to estimate the force acting on the bitumen-slide while being  
208 immersed or removed from probe liquid and used subsequently to determine the  
209 contact angle between bitumen and probe liquid.

210

211 The contact angle ( $\theta$ ) values are obtained by considering the equilibrium forces acting  
212 on the bitumen-coated slide while advancing and receding from the probe liquid using  
213 Eq. 3 (Bhasin, 2006):

214

$$215 \cos \theta = \frac{\Delta F + V_{im}(\rho_L - \rho_{air}g)}{P_t \gamma_L} \quad (3)$$

216

217 Where:  $P_t$  = perimeter of the bitumen coated plate

218  $\gamma_L$  = total surface energy of the probe liquid

219  $\Delta F$  = difference between weight of plate in air and partially submerged in  
220 probe liquid

221  $V_{im}$  = volume of solid immersed in the liquid

222  $\rho_L$  = density of the liquid

223  $\rho_{air}$  = air density

224  $g$  = gravitational force

225

226 To obtain surface energy values for the bitumen, contact angle values for at least three  
227 probe liquids are measured and applied to the Young-Dupré equation (Eq. 4) for the  
228 work of adhesion ( $W_{SL}$ ) between the two materials. Three equations are thus produced  
229 using the known surface energy components of the three probe liquids for the  
230 determination of the three surface energy components ( $\gamma^{LW}, \gamma^+, \gamma^-$ ) of the bitumen.

231

232  $W_{SL} = \gamma_L(1 + \cos \theta) = 2\sqrt{\gamma_S^{LW}\gamma_L^{LW}} + 2\sqrt{\gamma_S^-\gamma_L^+} + 2\sqrt{\gamma_S^+\gamma_L^-}$  (4)

233

234 Where subscripts L and S represents liquid and solid respectively, and  $\theta$  is the contact  
235 angle.

236

237 The resulting surface energy components for the five binders are presented in Table 1.  
238 The results for the 70/100 pen bitumen exhibited comparatively lower total surface  
239 energy ( $19.1 \text{ mJ/m}^2$ ) compared to the results for the 40/60 pen and 10/20 pen  
240 bitumens. However, in general all the results, including the anti-stripping modified  
241 binder (AAS1), are very similar.

242

243 Table 1. Surface energy characteristics of bitumen.

Bitumen	Surface energy components ( $\text{mJ/m}^2$ )			
	$\gamma^{LW}$	$\gamma^+$	$\gamma^-$	$\gamma$
10/20 pen	31.1	0.01	3.37	31.5
40/60 pen	30.6	0.00	2.40	30.6
70/100 pen	19.1	0.00	0.78	19.1
160/220 pen	28.2	0.00	0.30	28.8
AAS1	30.9	0.00	1.00	30.9

244

245 It is difficult to use the contact angle technique on high surface energy materials like  
246 aggregates (SFE values generally  $> 60 \text{ mJ/m}^2$ ) as probe liquids readily spread on high  
247 energy surfaces and it is difficult to obtain accurate contact angles. Therefore, for this  
248 part of the study a dynamic vapour sorption system (DVS Advantage 2, Surface  
249 Measurement Systems, Middlesex, UK) was used to determine sorption isotherms for  
250 the various aggregates and probe vapour combinations and the results used to  
251 determine the SFE components of the aggregate. The desired partial vapour pressures  
252 were varied from 0 to 95% with 5-10% increments (14 steps).

253

254 Five aggregates commonly used in UK asphalt mixtures were chosen for the study.  
255 The aggregates (two ‘limestones’ and three ‘granites’) were selected based on their  
256 difference in mineralogy and the fact that they exhibit different moisture damage  
257 performance (Airey et al., 2007). The mineralogy of the different aggregates was  
258 studied using a Mineral Liberation Analyser (MLA) in order to understand their  
259 morphology and to help with the overall analysis of results.

260

261 MLA comprises a procedure used to identify the mineral phases present in aggregates  
262 by combining a large specimen chamber automated Scanning Electron Microscope  
263 (SEM) and multiple Energy Dispersive X-ray detectors with automated quantitative  
264 mineralogy software. The software controls the SEM hardware to quantitatively  
265 analyse mineral and material samples. Automated stage control and image acquisition  
266 allows for rapid and systematic Back Scattered Electron (BSE) imaging and  
267 subsequent X-ray analysis of thousands of mineral grains and particles. Automatic  
268 recalibration ensures consistent results.

269

270 An FEI Quanta 600 SEM with MLA capability was used for the mineral phase  
271 determination. Aggregate samples were prepared by casting aggregates in resin,  
272 followed by polishing of the surface. The samples were then carbon coated to make  
273 them electron conductive and scanned in BSE mode with Electron Dispersive X-ray  
274 analysis (EDX) being carried out in an array of spots across the particles. The  
275 resultant spectra were then used to determine mineral phases at specific points in the  
276 microstructure which allowed mineralogical maps to be generated for each of the  
277 aggregate types (Grenfell et al., 2014).

278

279 Table 2. Mineral composition of aggregates obtained using MLA.

Mineral name	Composition (%)		
	Granite A	Granite B	Granite C
Quartz	19.11	15.86	33.17
Albite	27.13	32.73	28.30
K-feldspar	4.82	9.64	16.93
Chlorite	31.53	13.52	11.90
Muscovite	2.39	3.43	4.58
Other	0.74	1.91	1.19
Epidote	11.11	1.37	1.06
Biotite	0.99	0.34	1.00
Anorthite	0.10	18.54	0.82
Calcite	0.20	0.08	0.78
Hornblende	1.88	2.57	0.27
	Limestone A	Limestone B	
Calcite	96.98	98.94	
Dolomite	1.30	0.00	
Clay	0.93	0.37	
Quartz	0.49	0.55	
Other	0.30	0.13	

280 K-feldspar = potassium-dominant feldspar

281

282 The MLA results (in terms of mineral composition) for the five aggregates are  
283 presented in Table 2 and examples of the MLA scans for two of the aggregates

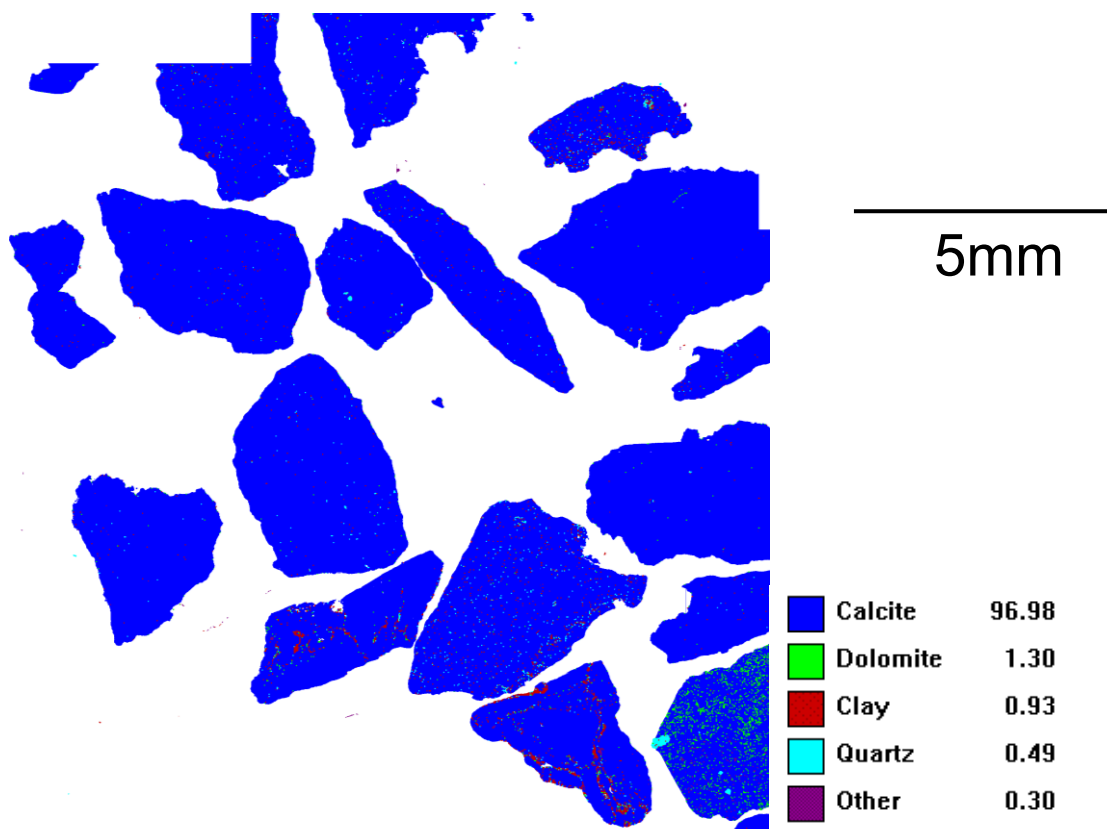
(Limestone A and Granite A) are presented in Figures 1 and 2. The results show that the aggregates have significantly different mineralogical make-up with Limestone A (Figure 1) being made up of predominantly (about 97%) calcite. Granite C, on the other hand, is made up of a number of different mineral phases with the predominant phase being quartz, but with significant quantities of albite and K\_feldspar (see Figure 2). It is believed that the large proportion of the quartz phase has the potential to lead to deleterious moisture properties, due to the poor adhesion between quartz and bitumen. However, there is also evidence that high feldspar content can be responsible for interfacial failure between bitumen and aggregate surfaces (Hognies et al., 2011).

293

In general, the limestone aggregates, being basic, are believed to perform better in practice as well as in moisture sensitivity tests, while the granite aggregates have been found to perform poorly in previous moisture sensitivity work (Grenfell et al., 2012).

297

298



299

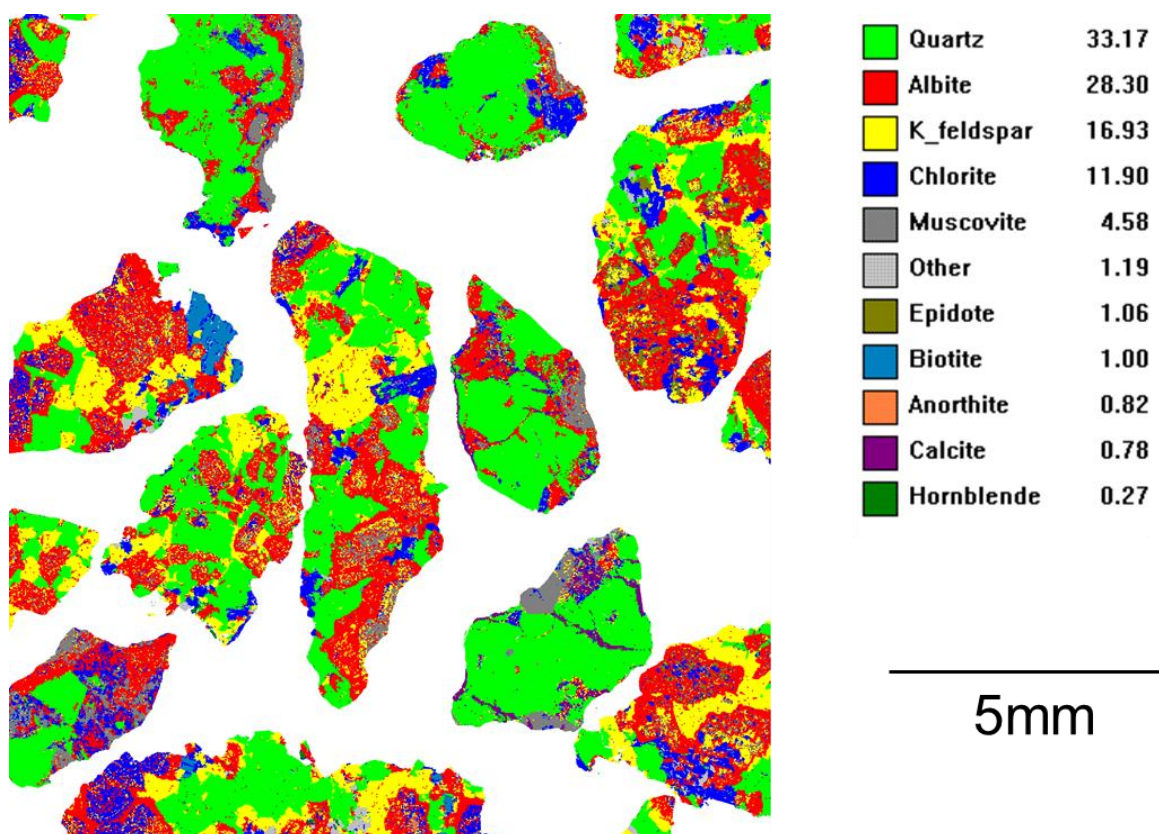
300

301 Figure 1. MLA analysis of Limestone A.

302

303 Prior to surface energy testing, the aggregates were first washed with deionised water  
304 and then dried in an oven to constant mass (up to 16 hours). An aggregate fraction  
305 passing 5mm and retained on 2.36mm was used. The upper limit on aggregate size is  
306 dictated by the material holding capacity of the DVS sample chamber. The cleaned  
307 oven-dried aggregate samples (less than 10 g) were again pre-heated in the DVS  
308 sample chamber at a temperature of 110°C for up to five hours to completely dry the  
309 samples before the sorption test.

310



311

312

313 Figure 2. MLA analysis of Granite C.

314

315 To perform the sorption test, carefully selected probe vapours (octane, ethyl acetate,  
316 and chloroform) with known SFE components were passed through the aggregate  
317 sample, under controlled temperature and partial vapour pressure conditions, with the  
318 aid of an inert carrier gas (nitrogen). The probes that were chosen for the aggregate  
319 testing had relatively low surface tension values as compared to the ones that are used  
320 for testing the bitumen to aid the ability to achieve a uniform adsorption/monolayer of  
321 the probe on the aggregate surface. Due to the surface characteristics of the aggregate,

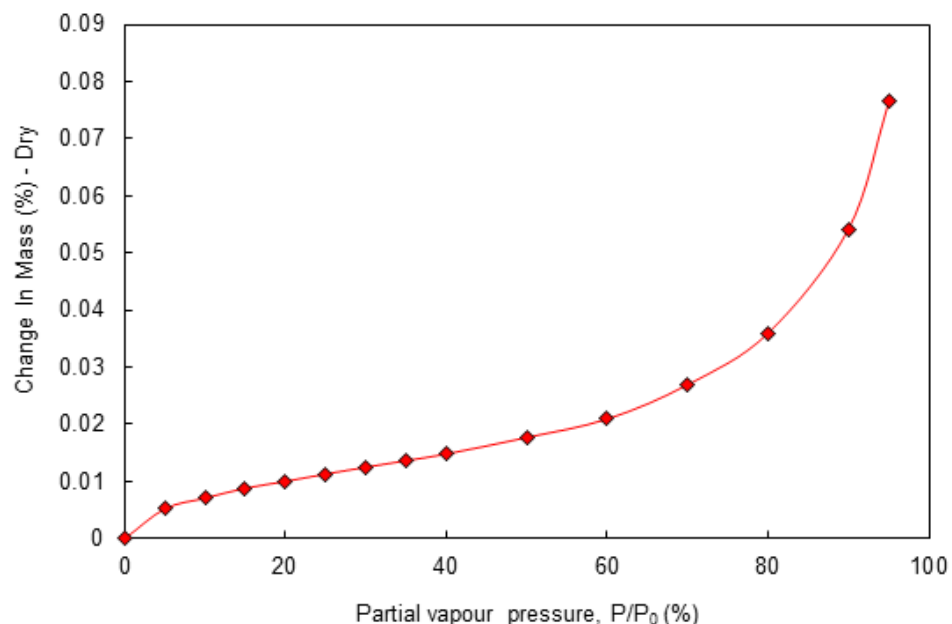
322 vapour probes get adsorbed on their surfaces which results in an increase in the mass  
323 of the aggregate sample that is then measured using a sensitive balance.

324

325 During the test, the aggregate material was exposed to different concentrations/vapour  
326 pressures of the probe liquids and the increase in mass of the aggregates, because of  
327 adsorption of the probe vapours on the aggregate surface, was measured. All the tests  
328 were performed at a temperature of 25°C. The change in mass of an aggregate sample  
329 was plotted against the increasing partial vapour pressure values to generate sorption  
330 isotherms which were used to estimate specific surface area and spreading equilibrium  
331 pressures of the aggregates.

332

333 A typical obtained adsorption isotherm is shown in Figure 3 for Limestone A  
334 aggregate with octane probe vapour for partial vapour pressures (concentrations)  
335 ranging from 0 to 95%. Similar isotherms were obtained for the other aggregates.



336

337 Figure 3. Typical sorption isotherm obtained for Limestone A aggregate using octane  
338 vapour as probe for partial vapour pressures (concentration) ranging from 0 to 95%  
339 with 5-10% increments (14 steps).

340

341 From Figure 3, it can be seen that the plot of adsorbed mass versus partial vapour  
342 pressures for Limestone A shows characteristics typical of Type II isotherms (Erbil,

343 2006). This suggests that the BET model can be used to fit the sorption isotherms (up  
344 to 35% partial vapour pressure) using the Langmuir approach (Eq. 5) where a plot of  
345  $P/(P_0 - P)n$  against  $P/P_0$  gives a straight line from which the BET constant ( $c$ ) and the  
346 specific amount of vapour adsorbed on the surface of aggregate ( $n_m$ ), can be obtained.  
347 The results were used to estimate the specific surface area of the aggregates using Eq.  
348 6 (Shaw, 1991; Sing, 1969).

349

350 
$$\frac{P}{n(P_0 - P)} = \left( \frac{c-1}{n_m c} \right) \frac{P}{P_0} + \frac{1}{n_m c} \quad (5)$$

351

352 Where:  $P$  = partial vapour pressure, Pa

353  $P_0$  = saturated vapour pressure of solvent, Pa

354  $n$  = specific amount adsorbed on the surface of the absorbent, mg; and

355  $c$  = BET constant (parameter theoretically related to the net molar enthalpy of  
356 the adsorption)

357

358 
$$SSA = \left( \frac{n_m N_o}{M} \right) \alpha \quad (6)$$

359

360 Where:  $SSA$  = specific surface area of solid,  $m^2$

361  $n_m$  = monolayer specific amount of vapour adsorbed on the aggregate surface,  
362 mg

363  $N_o$  = Avogadro's number,  $6.022 \times 10^{23} \text{ mol}^{-1}$

364  $M$  = molecular weight of the vapour, g/mol

365  $\alpha$  = projected or cross-sectional area of the vapour single molecule,  $m^2$

366

367 In addition to estimating the specific surface as previously described, the sorption  
368 isotherms were also used to calculate the spreading pressure which is required to  
369 determine surface energy components of the aggregates. Adsorption of vapour  
370 molecules on the aggregate surface reduces its SFE, so spreading pressure, as a result  
371 of adsorption of the vapour molecules, can be expressed as:

372

373 
$$\pi_e = \gamma_s - \gamma_{sv} \quad (7)$$

374 Where:  $\pi_e$  = spreading pressure at maximum saturated vapour pressure or equilibrium  
375 spreading pressure, mJ/m<sup>2</sup>

376  $\gamma_s$  = aggregate surface energy in vacuum

377  $\gamma_{sv}$  = aggregate surface energy after exposure to vapour

378

379 Spreading pressure at maximum saturation vapour pressure,  $\pi_e$ , for each solvent is  
380 calculated by using the following Gibbs free energy model (Eq. 8):

381

$$382 \quad \pi_e = \frac{RT}{A} \int_0^{P_o} \frac{n}{P} dP \quad (8)$$

383

384 Where:  $R$  = universal gas constant, 83.14 cm<sup>3</sup> bar/mol.K

385  $T$  = absolute temperature, K

386

387 By introducing spreading pressure,  $\pi_e$ , in the Young-Dupré relation (Eq. 4), the  
388 following relationship is obtained:

389

$$390 \quad W_{SL} = \pi_e + \gamma_{LV} (1 + \cos \theta) \quad (9)$$

391

392 The contact angle value for high energy solids such as aggregates is zero, therefore,  
393 Eq. 9 can be re-written as:

394

$$395 \quad W_{SL} = \pi_e + 2\gamma_{LV} \quad (10)$$

396

397 By substituting the above relation in Eq. 4, the following equation is obtained:

398

$$399 \quad 2\gamma_L + \pi_e = 2\sqrt{\gamma_S^{LW} \gamma_L^{LW}} + 2\sqrt{\gamma_S^+ \gamma_L^-} + 2\sqrt{\gamma_S^- \gamma_L^+} \quad (11)$$

400

401 From Eq. 11, if the spreading pressures from three different probe vapours are  
402 measured, then the three surface energy components of the aggregates ( $\gamma_S^{LW}, \gamma_S^+, \gamma_S^-$ )  
403 can be determined by solving three simultaneous equations.

404 For the five aggregates, only fractions passing the 5 mm sieve and retained on the  
405 2.36 mm sieve were tested and reported in this paper. The results were used to  
406 estimate specific surface area (SSA) and equilibrium pressure from which the surface  
407 energy parameters were calculated.

408

409 Specific surface area obtained for the five aggregates are presented in Table 3 using  
410 octane as the probe vapour. Specific surface area for the various aggregates showed  
411 large differences depending on aggregate type. The differences can be attributed to the  
412 different microstructure of the aggregates. The specific surface area obtained for each  
413 aggregate was used in two different ways: 1) to determine the equilibrium spreading  
414 pressure and 2) to calculate the moisture compatibility ratios.

415

416 Table 3. Surface energy characteristics of aggregates.

Aggregate	Surface energy components (mJ/m <sup>2</sup> )				SSA (m <sup>2</sup> /g)
	$\gamma^{LW}$	$\gamma^+$	$\gamma^-$	$\gamma$	
Limestone A	75.3	108.9	49.7	222.4	0.1708
Limestone B	66.3	2.9	4.9	73.8	0.7863
Granite A	69.1	17.3	568.3	267.4	0.3819
Granite B	68.3	16.4	40.8	120.0	0.3807
Granite C	68.0	163.9	122.7	351.6	0.4420

417

418 The SSA values were used to calculate the equilibrium spreading pressures on the  
419 aggregate surfaces for all three probes. Octane, being non-polar in nature, is supposed  
420 to give more accurate values of surface area (because non-polar substances do not  
421 have affinity for polar substances). The obtained spreading pressures were then used  
422 to compute the surface energy components ( $\gamma_s^{LW}, \gamma_s^+, \gamma_s^-$ ) as well as the total surface  
423 energy ( $\gamma_s$ ) for the aggregates as listed in Table 3.

424

425 The results show that surface energy properties vary considerably, in terms of surface  
426 energy components as well as total surface energy, amongst the different aggregates.  
427 The differences can be attributed to different elemental and mineralogical  
428 compositions of the aggregates. The test results indicate that there is not a significant  
429 difference between the van der Waals components of the aggregates (all  
430 approximately 70 mJ/m<sup>2</sup>) but there are significant differences between the acid-base  
431 components of the limestone and granite aggregates. On the basis of total surface  
432 energy alone, and for the same bitumen, Granite C ( $\gamma = 351.6$  mJ/m<sup>2</sup>) should

433 theoretically form stronger adhesive bond than Limestone B ( $\gamma = 73.8 \text{ mJ/m}^2$ ). Note  
434 that this assertion assumes a completely dry aggregate.

435

436 **2.3 Adhesion calculations**

437

438 The surface energy properties of the bitumen and the aggregates on their own have  
439 very little significance. However, when combined thermodynamically, they are  
440 helpful for estimating the interfacial work of adhesion between the two materials, with  
441 or without the presence of moisture.

442

443 The main objective for measuring surface energy of bitumen and aggregates is to be  
444 able to estimate the moisture sensitivity of asphalt mixtures using the principles of  
445 thermodynamics and physical adhesion. This objective was accomplished by using the  
446 surface energy properties of the aggregate and bitumen to calculate their interfacial  
447 work of adhesion (dry bond strength) and the reduction in free energy of the system  
448 (work of debonding) when water displaces bitumen from the aggregate-bitumen  
449 interface (Eqs 12 and 13). For an asphalt mixture to be durable and less sensitive to  
450 moisture, it is desirable that the work of adhesion between the bitumen and the  
451 aggregate be as high as possible.

452

453 In addition to the two parameters: dry bond strength and work of debonding, a third  
454 parameter, the cohesion of bitumen, can be calculated from the surface energy  
455 properties of bitumen. These three bond energy parameters (bitumen cohesion, dry  
456 bond strength, and work of debonding) can then be used to assess the moisture  
457 sensitivity of an asphalt mixture. Bitumen cohesion is the cohesive bond strength of  
458 the material and is estimated as twice the total surface energy of the material. Dry  
459 bond strength ( $W_{BA}^a$ ) is defined as given in Eq. 12 as the interfacial work of adhesion  
460 between the bitumen ( $B$ ) and aggregate ( $A$ ). A higher value of dry bond strength  
461 suggests greater adhesion between the two materials and hence more resistance  
462 against debonding.

463

464 
$$W_{BA}^a = 2\sqrt{\gamma_B^{LW}\gamma_A^{LW}} + 2\sqrt{\gamma_B^+\gamma_A^-} + 2\sqrt{\gamma_B^-\gamma_A^+} \quad (12)$$

465

466 Eq. 13 gives the work of debonding ( $W_{BWA}^a$ ) which is considered as the reduction in  
 467 bond strength of a bitumen-aggregate system when water ( $W$ ) is introduced into the  
 468 system or when water displaces the bitumen from the aggregate surface. This quantity  
 469 might also be interpreted as the energy required for water to separate or break the  
 470 bond of bitumen-aggregate systems.

471

472 In general, ( $W_{BWA}^a$ ) is found to be a negative value for most aggregate-bitumen  
 473 systems. This means that the process of water breaking or separating the existing  
 474 adhesive aggregate-bitumen bond is a thermodynamically favourable process. In other  
 475 words, no external work is required for this separation process to occur once water  
 476 reaches the aggregate-bitumen interface. A smaller absolute value of this parameter  
 477 for a given bitumen-aggregate system is indicative of a better moisture damage  
 478 performance of that system.

479

$$W_{BWA}^a = \left\{ \left( (\sqrt{\gamma_A^{LW}} - 4.67)^2 \right) + \left( 2 \times (\sqrt{\gamma_A^+} - 5.05) \times (\sqrt{\gamma_A^-} - 5.05) \right) \right\}$$

480  $+ \left\{ \left( (\sqrt{\gamma_B^{LW}} - 4.67)^2 \right) + \left( 2 \times (\sqrt{\gamma_B^+} - 5.05) \times (\sqrt{\gamma_B^-} - 5.05) \right) \right\}$

 $- \left\{ \left( (\sqrt{\gamma_B^{LW}} - \sqrt{\gamma_A^{LW}})^2 \right) + \left( 2 \times (\sqrt{\gamma_B^+} - \sqrt{\gamma_A^+}) \times (\sqrt{\gamma_B^-} - \sqrt{\gamma_A^-}) \right) \right\}$ 

(13)

481

482 Work of adhesion results for the various aggregate-bitumen combinations are  
 483 presented in Table 4. The results show both the influence of the different aggregates  
 484 and bitumen on work of adhesion.

485

486 Table 4. Work of adhesion between bitumen and aggregates.

Bitumen	Work of adhesion (mJ/m <sup>2</sup> )				
	Limestone A	Limestone B	Granite A	Granite B	Granite C
10/20 pen	136	98	113	108	141
40/60 pen	128	95	105	104	131
70/100 pen	94	74	80	79	95
160/220 pen	104	88	93	92	102
AAS1	117	94	101	100	117

487

488 Work of debonding values for the aggregate-bitumen combinations are presented in  
 489 Table 5.

490 Table 5. Work of debonding in the presence of water.

Bitumen	Work of debonding (mJ/m <sup>2</sup> )				
	Limestone A	Limestone B	Granite A	Granite B	Granite C
10/20 pen	-47	56	-174	-32	-103
40/60 pen	-51	58	-177	-35	-109
70/100 pen	-67	55	-185	-52	-128
160/220 pen	-64	63	-177	-16	-126
AAS1	-57	62	-176	-13	-117

491

492 In addition to the work of adhesion, the greater the magnitude of work of debonding  
 493 when water displaces bitumen from the aggregate-bitumen interface (in terms of  
 494 absolute values of this quantity), the greater will be the thermodynamic potential that  
 495 drives moisture damage. Granite A and Granite C therefore have a far greater  
 496 potential for moisture damage compared to the limestone aggregates and Granite B. In  
 497 addition, the positive values for Limestone B indicate that external work or energy  
 498 would be required for water to be able to separate the existing adhesive bond between  
 499 the different binders and this aggregate. In other words, of all the aggregate-bitumen  
 500 combinations, those with Limestone B have the greatest potential resistance to  
 501 debonding caused by water.

502

503 The results also show that for a given aggregate, work of debonding (absolute values)  
 504 generally increases slightly (in magnitude) for softer bitumen compared to harder  
 505 (stiffer) binders. This is true for Limestone A and B as well as Granite C although the  
 506 results for Granite A are fairly consistent for all four penetration grade bitumens and  
 507 there is a considerable decrease in absolute value for the soft 160/220 pen bitumen for  
 508 Granite B.

509

#### 510     **2.4 Adhesion bond energy parameters**

511

512 The ratio ( $ER_1$ ) between the adhesive bond energy values in the dry condition ( $W_{BA}^a$ )  
 513 and in the presence of water ( $W_{BWA}^a$ ) can be used to predict the moisture sensitivity of  
 514 asphalt mixtures. A higher value of energy ratio indicates better resistance to moisture  
 515 damage for that bitumen-aggregate combination. Bhasin et al. (2006) used energy  
 516 ratio  $ER_1$  to study different types of asphalt mixtures and concluded that mixtures with  
 517 a ratio higher than 1.5 were more moisture resistant than the ones with ratios lower  
 518 than 0.8.

519      
$$ER_1 = \left| \frac{W_{BA}^a}{W_{BWA}^a} \right| \quad (14)$$

520  
 521 Aggregates with higher surface roughness and greater surface area are supposed to  
 522 bond better with bitumen by providing more bond area and better interlocking. In  
 523 order to accommodate this effect, a second bond energy parameter ( $ER_1 * SSA$  or  $ER_3$ )  
 524 obtained by multiplying the bond energy ratio ( $ER_1$ ) with specific surface area (SSA)  
 525 has been proposed in addition to  $ER_1$  to predict moisture sensitivity of asphalt  
 526 mixtures (Bhasin et al., 2006).

527  
 528 Wetting/coating of an aggregate with bitumen is not only affected by the surface  
 529 properties of the two materials; the viscosity or cohesion of the bitumen itself also  
 530 plays a very important role. Bitumen with lesser cohesion and greater affinity for the  
 531 aggregates will have a higher wettability and will coat the aggregate surface more  
 532 than bitumen having lesser wettability characteristics. However, softer bitumen  
 533 having lesser cohesion may be more prone to emulsification (decrease in cohesion) in  
 534 the presence of water. The effects of cohesion and wettability on moisture resistance  
 535 can be accounted for by modifying the  $ER_1$  parameter by replacing the bond strength  
 536 in the dry condition ( $W_{BA}^a$ ) with a wettability relationship ( $W_{BA}^a - W_{BB}$ ). This new  
 537 moisture sensitivity assessment parameter ( $ER_2$ ) is given in Eq. 15 (Bhasin, 2006). In  
 538 order to accommodate the effects of aggregate micro-texture on the bitumen-  
 539 aggregate bond strength in the presence of moisture, the bond parameter  $ER_2$  can be  
 540 multiplied by specific surface area of the aggregates to obtain a fourth bond energy  
 541 parameter ( $ER_2 * SSA$  or  $ER_4$ ) (Bhasin, 2006).

542  
 543 
$$ER_2 = \left| \frac{W_{BA}^a - W_{BB}}{W_{BWA}^a} \right| \quad (15)$$

544  
 545 Where ( $W_{BA}^a$ ) and ( $W_{BB}$ ) represent bitumen-aggregate dry bond strength and bitumen  
 546 cohesion respectively.

547  
 548 These four bitumen-aggregate bond energy parameters ( $ER_1$ ,  $ER_2$ ,  $ER_3$  and  $ER_4$ ) were  
 549 used to assess the moisture susceptibility of the asphalt mixtures. In all cases, higher

550 energy ratios are associated with mixtures with better moisture resistance. It is  
 551 important to note that the energy ratios have been developed for aggregate-binder  
 552 systems that demonstrate a negative value for the work of adhesion under 'wet'  
 553 conditions ( $W_{BWA}^a$ ) and are therefore are not applicable for the systems containing  
 554 Limestone B which produced positive values of  $W_{BWA}^a$  as shown in Table 5.

555

556 Table 6 shows the aggregate-bitumen bond energy parameters (ER<sub>1</sub>, ER<sub>2</sub>, ER<sub>3</sub> and  
 557 ER<sub>4</sub>) for the asphalt mixtures (bitumen-aggregate combinations). Values have been  
 558 included for the aggregate-bitumen combinations containing Limestone B although,  
 559 as explained above, they do not represent the actual resistance of the mixture to  
 560 moisture damage.

561

562 Table 6. Bond energy parameters for aggregate-bitumen combinations.

Bitumen	Limestone A	Limestone B	Granite A	Granite B	Granite C	Threshold criteria <sup>a</sup>
ER <sub>1</sub>						
10/20 pen	2.90	1.74 <sup>b</sup>	0.65	3.41	1.37	$\geq 0.75$
40/60 pen	2.52	1.64 <sup>b</sup>	0.59	2.93	1.20	
70/100 pen	1.40	1.36 <sup>b</sup>	0.43	1.54	0.74	
160/220 pen	1.63	1.40 <sup>b</sup>	0.52	5.81	0.81	
AAS1	2.07	1.52 <sup>b</sup>	0.57	7.86	1.00	
ER <sub>2</sub>						
10/20 pen	1.56	0.62 <sup>b</sup>	0.29	1.86	0.76	$\geq 0.50$
40/60 pen	1.32	0.59 <sup>b</sup>	0.25	1.56	0.64	
70/100 pen	0.83	0.66 <sup>b</sup>	0.23	0.94	0.44	
160/220 pen	0.74	0.51 <sup>b</sup>	0.21	2.26	0.36	
AAS1	0.98	0.52 <sup>b</sup>	0.22	3.00	0.47	
ER <sub>3</sub>						
10/20 pen	0.49	1.37 <sup>b</sup>	0.25	1.30	0.61	$\geq 0.50$
40/60 pen	0.43	1.29 <sup>b</sup>	0.23	1.12	0.53	
70/100 pen	0.24	1.07 <sup>b</sup>	0.17	0.59	0.33	
160/220 pen	0.28	1.10 <sup>b</sup>	0.20	2.21	0.36	
AAS1	0.35	1.19 <sup>b</sup>	0.22	2.99	0.44	
ER <sub>4</sub>						
10/20 pen	0.27	0.49 <sup>b</sup>	0.11	0.71	0.34	$\geq 0.35$
40/60 pen	0.22	0.46 <sup>b</sup>	0.09	0.59	0.28	
70/100 pen	0.14	0.52 <sup>b</sup>	0.09	0.36	0.20	
160/220 pen	0.13	0.40 <sup>b</sup>	0.08	0.86	0.16	
AAS1	0.17	0.41 <sup>b</sup>	0.08	1.14	0.21	

563

<sup>a</sup>after Little and Bhasin (2006)

564

<sup>b</sup>Computed but not applicable for moisture damage assessment

565

566 It is worth reiterating that the energy ratios used in this paper and presented in Table 6  
567 are based on absolute values. These ratios therefore do not take into account  
568 differences in the thermodynamic processes associated with debonding caused by  
569 water which means that all four bond energy ratios treat all five aggregates the same.  
570 Clearly this is not the case with Limestone B showing a positive value for the work of  
571 debonding ( $W_{BWA}^a$ ) compared to the negative values obtained for the other four  
572 aggregates. This implies that all combinations with this aggregate should have higher  
573 energy ratios than those reported in Table 6 in order to reflect the greater resistance to  
574 debonding in the presence of water. As this has not been done in the paper, it is  
575 important to consider the energy ratio results for Limestone B as conservative values.  
576

577 The four bond energy parameters can be used to predict the moisture sensitivity of  
578 asphalt mixtures using threshold values defined to separate ‘good’ from ‘poor’  
579 moisture damage performing aggregate-bitumen combinations. The threshold limits  
580 are 0.75 for ER<sub>1</sub>, 0.50 for ER<sub>2</sub>, 0.50 for ER<sub>3</sub> and 0.35 for ER<sub>4</sub> (Bhasin, 2006; Bhasin  
581 et al., 2006; Little and Bhasin, 2006). Once again, the criteria given by Bhasin to  
582 differentiate between ‘good’ and ‘poor’ performing mixtures were obtained using data  
583 in which all aggregate-binder combinations had negative values of work of adhesion  
584 in the presence of water and are therefore are not applicable for any of the  
585 combinations with Limestone B.

586  
587 In general the limestone aggregate-bitumen combinations tend to have higher values  
588 compared to the granite aggregate-bitumen combinations although the values for  
589 Granite B, especially ER<sub>1</sub> and ER<sub>2</sub>, are very high. The results show that the ranking of  
590 the ‘good’ versus ‘poor’ moisture damage performing aggregate-bitumen  
591 combinations for ER<sub>1</sub> and ER<sub>2</sub> are quite similar; both parameters placing the same  
592 number of combinations in ‘good’ versus ‘poor’ categories. The results for the other  
593 two parameters, ER<sub>3</sub> and ER<sub>4</sub>, are also similar but the later placed more mixtures in  
594 the ‘poor’ category. The results suggest, for the materials considered, that ER<sub>1</sub> and  
595 ER<sub>2</sub> are sensitive to binder cohesion as the softer 70/100 pen bitumen showed lower  
596 ratios irrespective of the aggregate type. In addition, the use of an anti-stripping  
597 additive (binder AAS1) has not appeared to affect the bond energy ratios compared to

598 those found for the 40/60 pen base bitumen with the only exception being the values  
599 for Granite B which showed a significant increase.

600

601 Compared to the ER<sub>1</sub> and ER<sub>2</sub> parameters, the results for ER<sub>3</sub> and ER<sub>4</sub> show the  
602 significant influence of SSA on the selection of ‘good’ versus ‘poor’ moisture damage  
603 performing aggregate-bitumen combinations. Because of the apparent large influence  
604 of SSA on moisture sensitivity of asphalt mixtures shown in Table 6, the bond  
605 parameters ER<sub>3</sub> and ER<sub>4</sub> appear to be more suitable indices for determining the  
606 performance of the different aggregate-bitumen combinations with a clear distinction  
607 in terms of ‘good’ and ‘poor’ aggregates.

608

### 609     **3. Aggregate-bitumen stripping**

610

611 The same five aggregates (two limestones and three granites) and two of the binders  
612 (40/60 pen and 160/220 pen) were tested using the four aggregate-bitumen stripping tests.  
613 In addition, the anti-stripping modified binder AAS1 was also used with the five  
614 aggregates but only for two of the aggregate-bitumen stripping tests due to shortages in  
615 the supply of the amine-based anti-stripping agent. Based on field experience, the  
616 limestone aggregates tend to be more resistant to moisture damage than the granite  
617 aggregates. Therefore, it was expected that a discriminating laboratory test should be able  
618 to distinguish between the mixtures based on the selected aggregates.

619

620 In most of the existing test standards for evaluating moisture resistance of loose asphalt  
621 mixtures, the most commonly used aggregate sizes range from 6.3 mm to 9.5 mm.  
622 Therefore, for each of the five aggregate types selected for testing, only material passing  
623 the 9.6 mm sieve size but retained on the 6.3 mm sieve was used.

624

#### 625     **3.1 Static immersion test**

626

627 The static immersion test was conducted in accordance with ASTM D1664 (AASHTO  
628 T182). During the test, a 100 g sample of aggregate with sizes ranging from 6.3 to 9.5  
629 mm coated with 5.5 g of bitumen was immersed in distilled water at 25°C for 16 to 18  
630 hours in a 500 ml glass bottle. The sample was then observed through the glass to  
631 estimate the percentage of total visible area of aggregate that remains coated as above or

632 below 95%. Three replicate 100 g aggregate samples coated with bitumen were tested  
633 and the average percentage coated estimated. Some of the disadvantages of the test are 1)  
634 the test is subjective and therefore has high variability and, 2) the test does not involve  
635 any strength tests that directly relate to mixture performance.

636

637 The results in terms of percentage of total visible area of aggregate that remains coated  
638 after 16 to 18 hours of soaking are presented in Figure 4. The results indicated that 100%  
639 of the aggregate remained coated at the end of the test for all the limestone aggregate  
640 mixtures. For the granite mixtures, the percentage coated area observed for each  
641 aggregate was above 95% with the exception of Granite C that showed about 90% coated  
642 area.

643

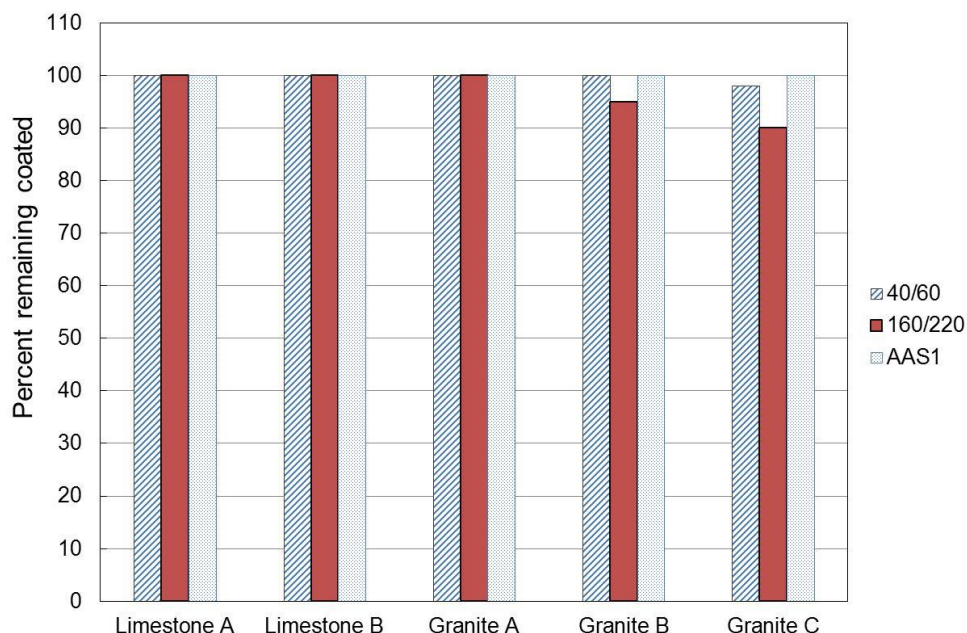


Figure 4. Percent aggregate coating after static immersion test

658

659 The results suggest that most of the aggregate/binder combinations showed similar  
660 bonding (greater than 95% of coated aggregates) properties after undergoing the static  
661 immersion test. The exception was the combinations of Granite C which showed a 10%  
662 striped aggregate result with the 160/220 pen bitumen. Granite B showed a 5% stripping  
663 value with the 160/220 pen bitumen. These results are in agreement with previous studies  
664 (Vuorinen and Hartikainen, 2001; Liu et al., 2014) that used similar aggregates. Results  
665 for the mixtures containing amine-based anti-stripping agents with retained binder greater

666 than 95% appear to be in agreement with previous research (Ahmad 2011). Even though  
667 the static immersion test ranked the Granite C - 60/200 pen combination as worst in terms  
668 of moisture sensitivity, the test appears not to be sensitive to the different aggregate types  
669 as it ranked the remaining aggregates with all the binders, except 160/220 pen, equally.

670

671 **3.2 Rolling bottle test**

672

673 The rolling bottle test (RBT) was conducted in accordance with BS EN 12697-11  
674 (Bituminous mixtures - Test methods for hot mix asphalt part 11 - Determination of the  
675 affinity between aggregate and bitumen). The RBT is a subjective test in that affinity is  
676 expressed by visual estimation of the degree of bitumen coverage on uncompacted  
677 bitumen-coated mineral aggregate particles after the influence of mechanical stirring  
678 action in the presence of water. To perform the test, dust-free aggregate samples  
679 weighing 170 g were dried in an oven at  $105\pm 5^{\circ}\text{C}$  overnight to constant mass and then  
680 coated with 5.7 g of molten binder. Mixing of the aggregates with binder was conducted  
681 at  $120\pm 5^{\circ}\text{C}$ . The aggregate-binder mixture was then cooled loose at room temperature.  
682 The loose mixture was stored at ambient temperature for 12 to 64 hours before testing.  
683 Each of the test bottles were filled to about half their volume with deionized water and  
684 about 150 g of the loose aggregate-mixture was placed in each bottle. The whole  
685 assembly was put in the bottle roller rotating at a speed of 60 rotations per minute for six  
686 hours. At the end of the six-hour period, the aggregate particles were emptied from the  
687 test bottle into a test bowl which was then filled with fresh, de-ionized water to a level  
688 just above the top of the surface of the particles. Subsequently, the test bowl was placed  
689 on a white surface. The purpose of adding fresh water was to allow for optimal visual  
690 determination of binder coverage on the aggregate particles. At least three replicates of  
691 each sample were tested.

692

693 At the end of the test, the degree of bitumen coverage of the aggregate particles was  
694 estimated by visual observation and recorded to the nearest 5%. The degree of bitumen  
695 coverage was defined as the average proportion of the surface area of the aggregate  
696 particles covered with bitumen, expressed as a percentage (equal to 100 minus the  
697 percentage of stripping). The procedure (i.e. rotation in the bottle roller and measuring of  
698 bitumen coverage) was repeated for three more cycles (24 hours, 48 hours, and 72 hours)  
699 with fresh water replacing the fouled water in the test bottle at the end of each cycle and

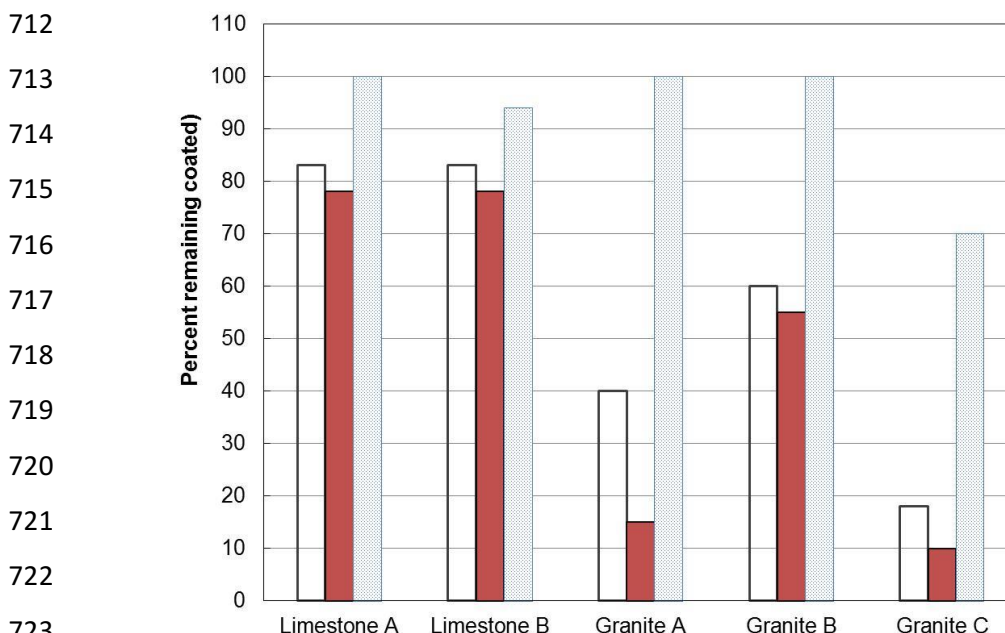
700 the degree of bitumen coverage being measured. For each rolling time (6, 24, 48, and 72  
701 hours), the mean value for each repeat was calculated to the nearest 5% and the results  
702 averaged to obtain the average degree of bitumen coverage for a given mixture.

703

704 Mixtures containing the unmodified binders showed higher binder loss than the modified  
705 binder containing anti-striping agent. Binder losses in the mixtures containing the  
706 160/220 pen binder were highest for each aggregate type tested (Figure 5). Binder losses  
707 in the 40/60 pen mixtures were just slightly less than 160/220 pen binder although both  
708 were higher than the mixtures containing anti-striping agent for all of the aggregates  
709 considered.

710

711



725 Figure 5. Percent aggregate coating after 72 hours of RBT

726

727 The results show that the rolling bottle test is sensitive to changes in aggregate and binder  
728 property including binder modification. Compared to the static immersion test, the rolling  
729 bottle appears more discriminatory as it was able to show small differences in moisture  
730 susceptibility in the good performing limestone aggregates. For example, ranking in this  
731 case was (in increasing order of resistance) 160/220 pen, 40/60 pen and amine-based anti-  
732 stripping agent, which was to be expected.

733

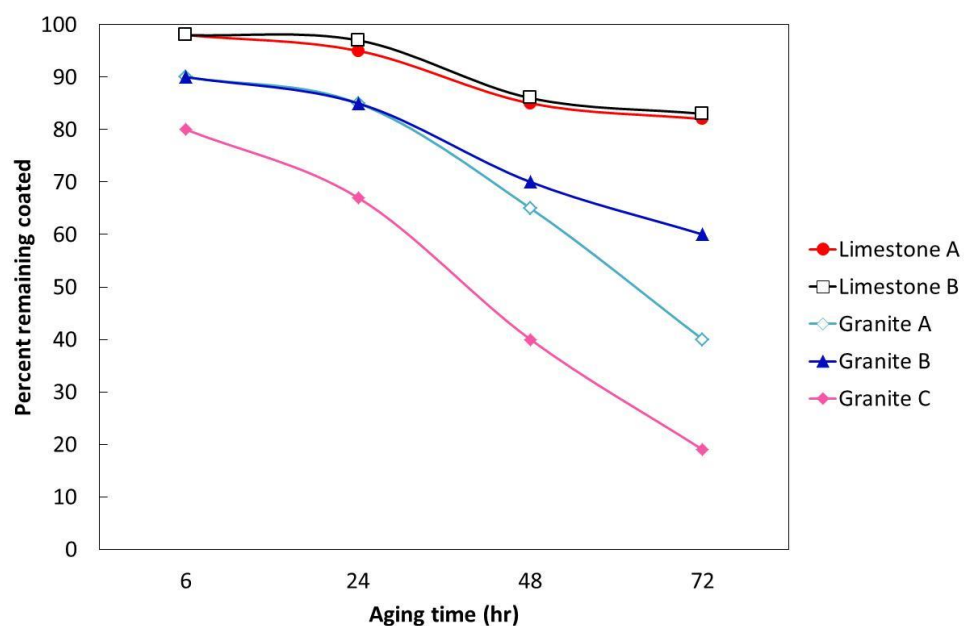
734 Compared to the static immersion test, the sensitivity of the rolling bottle test was higher.  
735 Figure 6 shows the binder loss versus conditioning time obtained for mixtures containing  
736 40/60 pen binder that illustrates the sensitivity of the rolling bottle test to different  
737 aggregate types. The limestone aggregates (Limestone A and B) perform better than the  
738 granite aggregates (Granite A, B and C). The results showing Granite C as the worst  
739 performing aggregate again are as expected based on field performance.

740

741 From the curves in Figure 6, it could be seen that the percentages of bitumen coverage  
742 decreased slowly with testing time for limestone, while on the contrary, percentages  
743 for granite reduce sharply during the test period. For instance, during the first six  
744 hours, Limestone B showed only a 2% binder loss while Granite C showed about 20%  
745 loss. In addition, the percentage of binder loss for Granite C at 6 hours is equal to that  
746 for the limestone aggregates at 72 hours. Among the granite aggregates, Granite B  
747 showed the best bonding properties as illustrated by the 10%, 15%, 30%, 40% of  
748 binder loss for 6, 24, 48 and 72 hours, respectively. Although the total loss of binder  
749 for Granite A was more than Granite B, these two aggregate had almost the same  
750 percentage of binder loss after the first 24 hours. Similar results were obtained for the  
751 softer 160/220 pen binder.

752

753



766 Figure 6. Kinetics of bitumen coverage of aggregates during RBT

767

768    3.3    ***Boiling Water Test***

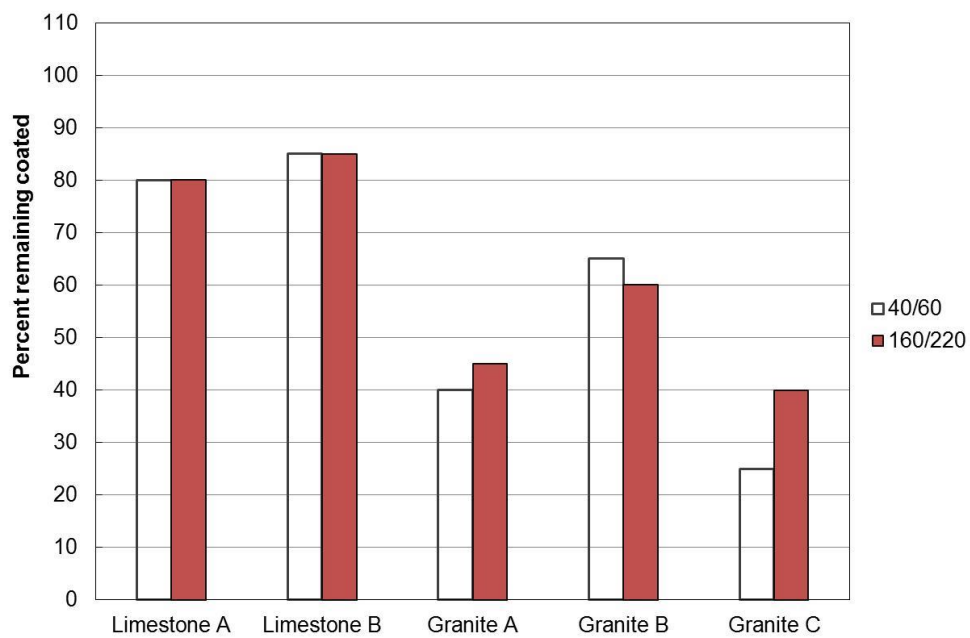
769

770    The boiling water test was performed in accordance with ASTM D3625 - 96(2005)  
771    (Standard Practice for Effect of Water on Bituminous-Coated Aggregate Using Boiling  
772    Water). Compared with the static immersion and rolling bottle tests, the boiling water  
773    test is a quicker approach to evaluate the moisture sensitivity of the bitumen and  
774    aggregate combination since it only takes about 60 minutes to condition the sample  
775    compared with more than 72 hours for the rolling bottle test or 16 to 18 hours in the case  
776    of the static immersion test. Like the static immersion test, the boiling water test cannot  
777    be used as a measure of field performance because such correlations have not been  
778    established. At least three replicates of each sample were tested.

779

780    To perform the test, 600 g of clean oven-dried aggregates were fully coated with 30 g of  
781    molten binder. About 300 g each of the aggregate-bitumen mixture was submerged under  
782    boiling water in a glass beaker and the mixture boiled for 10 minutes. The percentage of  
783    the total visible area of the aggregate that retained its original coating of bitumen was  
784    used as an estimate of moisture damage. Only two binders (40/60 pen and 160/220 pen)  
785    were evaluated using the boiling water test.

786



800    Figure 7. BWT results for different aggregate-bitumen systems

801

802 The results are shown in Figure 7 where Granite C again exhibited the worst bonding  
803 properties. Considering the limestone aggregates, the performance of Limestone A and B  
804 was similar for both 40/60 pen and 160/220 pen binder. In terms of the granite  
805 aggregates, the 160/220 pen binder showed better bond performance than the 40/60 pen  
806 binder except for Granite A.

807

### 808 **3.4 Total Water Immersion Test**

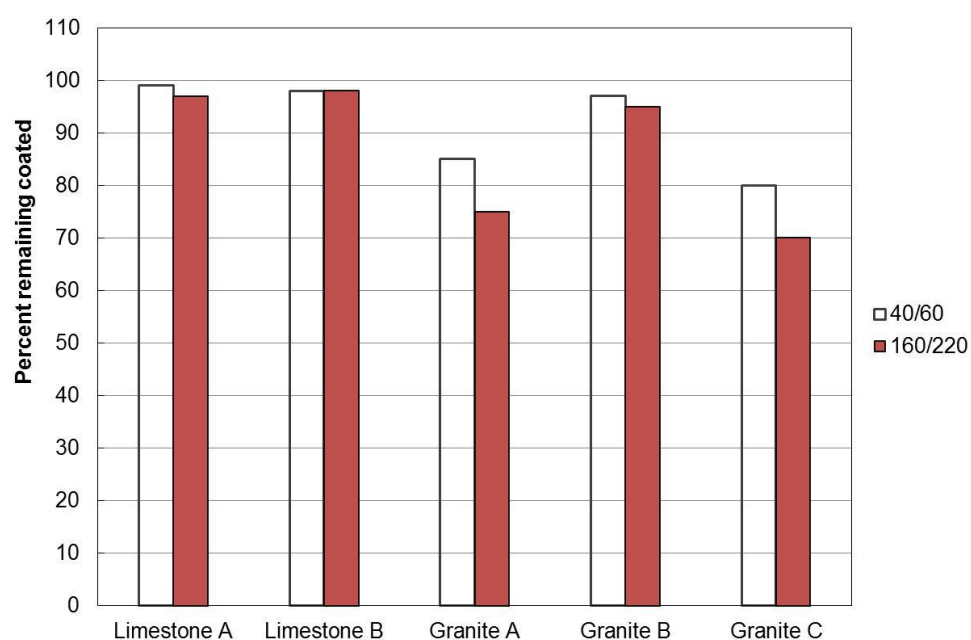
809

810 The total water immersion test (TWIT) was performed in the laboratory to compare the  
811 performance of bitumen doped with an adhesion agent against the non-doped bitumen.  
812 This is necessary to check each aggregate with non-doped and doped bitumen to assess  
813 the effectiveness of the additive or whether the aggregate needs additive in the binder to  
814 provide proper adhesion. Three replicates of each sample were tested.

815

816 The test assesses the average percentage of binder coverage after immersion in 40°C  
817 water after 3 hours of soaking. The test is an improvement on the static immersion test. It  
818 uses water at 40°C rather than room temperature (25°C) used in the static immersion test  
819 to provide a better result. Again only two binders (40/60 pen and 160/220 pen) were  
820 evaluated using the total water immersion test.

821



836 Figure 8 shows the average percentage of binder coverage after immersion in 40°C water  
837 for 3 hours obtained during the total water immersion test. From Figure 8, it can be seen  
838 that the limestone aggregates had very little binder loss compared with the granite  
839 aggregates. The percentages of binder loss for limestone were all less than 5% for the two  
840 binder types. The results for the granite aggregates showed higher percentages of binder  
841 loss. As in the previous stripping tests, Granite C showed the worst performance with  
842 20% and 30% binder loss, for 40/60 pen and 160/220 pen, respectively.

843

#### 844 4. Asphalt mixture moisture conditioning using the SATS procedure

845

846 SATS is the first procedure of its kind that combines both ageing and water damage  
847 mechanisms (subjected to asphalt pavements in service) within a single laboratory test  
848 protocol. The procedure has been found to successfully reproduce the moisture  
849 damage observed in asphalt materials in the field (Collop et al. 2004a) as well as  
850 distinguish between poor performing material and alternative asphalt mixtures  
851 incorporating aggregate with good durability track records (Choi et al, 2002, Airey et  
852 al. 2003, Collop et al. 2004b and Choi, 2005). The results obtained from the SATS  
853 moisture conditioning procedure tend to rank asphalt mixtures in terms of moisture  
854 sensitivity in the same order as the AASHTO T283 procedure (Anon, 2000), although  
855 the relative performance of a mixture containing a moisture sensitive aggregate is  
856 usually significantly lower in the SATS test (Airey et al., 2005).

857

858 The standard SATS procedure involves conditioning five pre-saturated specimens  
859 simultaneously in a pressure vessel under 0.5 MPa air pressure at a temperature of  
860 85°C for a period of 24 hours. This conditioning is followed by a cooling period of 24  
861 hours before the air pressure is released and the vessel opened to remove the  
862 specimens for stiffness testing (Grenfell et al., 2012). The pressure vessel used can  
863 hold five nominally identical specimens (100 mm in diameter and 60 mm in  
864 thickness) in a custom-made specimen tray. The dimensions and specifications of the  
865 SATS testing equipment, including the size and spacing of the holes in the perforated  
866 trays are detailed in Clause 953 of Volume 1 of the UK Manual of Contract  
867 Documents for Highway Works, 2004 (MCHW, 2004). The conditions used with the  
868 SATS procedure were selected in order to reproduce in the laboratory, the field  
869 observed moisture damage as demonstrated by a decrease in stiffness modulus for

870 particular asphalt mixtures as detailed by Airey *et al.* (2005). The key features of the  
871 conditioning procedure can be summarised as follows:

872

- 873 • A well-insulated, heated pressure vessel capable of holding five compacted  
874 asphalt specimens (100 mm diameter × 60 mm height).
- 875 • Conditioning set-up allowing simultaneous pressure and temperature control.
- 876 • Asphalt specimens, which have been pre-saturated with water (under vacuum),  
877 located on a purpose-built tray.
- 878 • A pre-determined quantity of water placed in the vessel so that the bottom  
879 specimen is fully immersed during the conditioning procedure.
- 880 • Simultaneous conditioning of five specimens under 0.5 MPa air pressure at a  
881 temperature of 85°C for 24 hours, followed by a cooling-down period of 24  
882 hours before the pressure is released and the vessel opened to remove the  
883 specimens for stiffness testing.

884

885 The ten steps of the SATS conditioning and test procedure as specified in Clause 953  
886 are as follows:

887

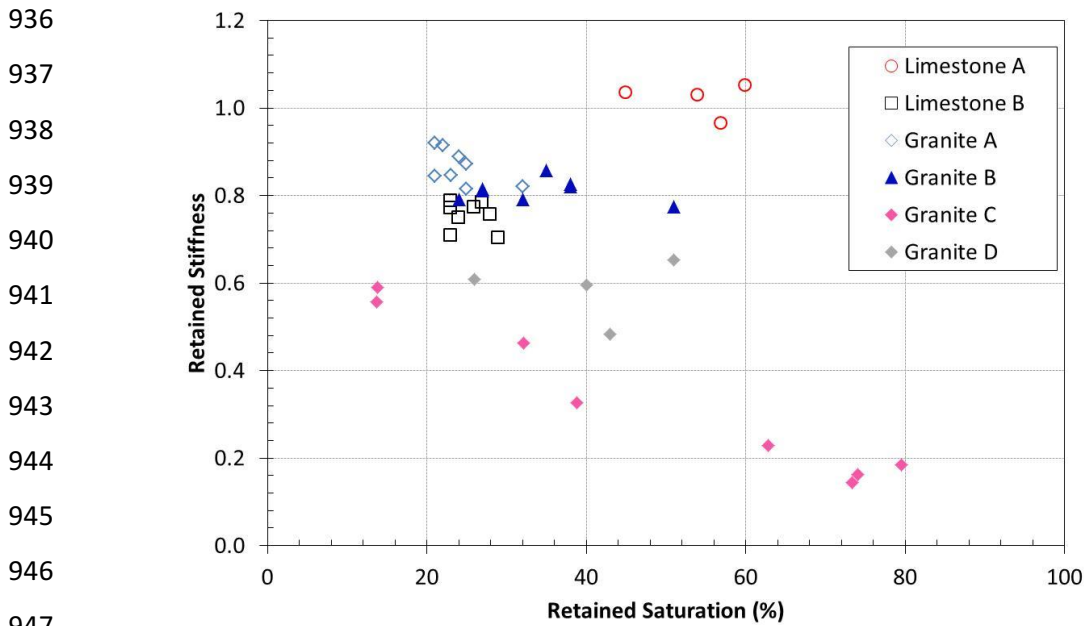
- 888 1. The unconditioned (initial) indirect tensile stiffness modulus of each asphalt  
889 mixture specimen is determined at 20°C using the Nottingham Asphalt Tester  
890 (NAT) (Cooper and Brown, 1989) in accordance with BS EN 12697-26 Annex  
891 C (124msec rise time, 5µm peak transient horizontal diametral deformation)  
892 (BSI 2004a).
- 893 2. The dry mass of each specimen is determined by weighing.
- 894 3. The specimens are subsequently immersed in distilled water at 20°C and  
895 saturated using a residual pressure of 35 kPa (i.e. 65 kPa below atmospheric  
896 pressure) for 30 minutes.
- 897 4. The wet mass of each specimen is determined by weighing, and the percentage  
898 saturation of each specimen calculated, referred to as ‘initial saturation’.
- 899 5. The SATS pressure vessel is partly filled with a pre-determined amount of  
900 distilled water (final water level between the bottom, submerged specimen and  
901 the above ‘dry’ (pre-saturated specimen)). The pressure vessel and water are

maintained at the target temperature of 85°C for at least 2 hours prior to introducing the specimens.

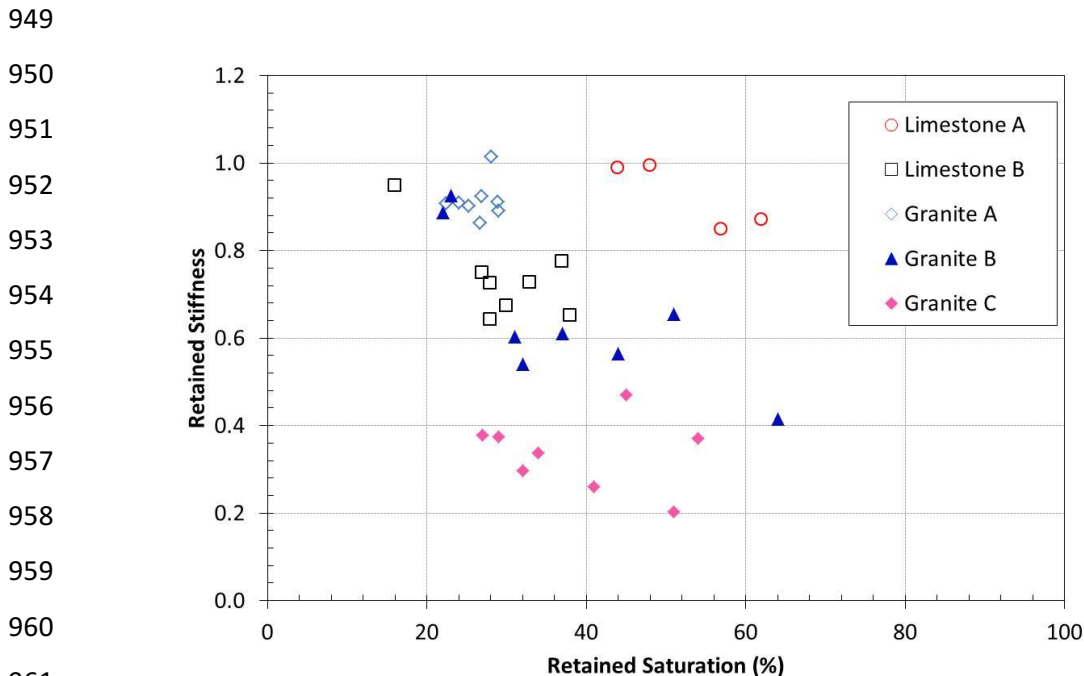
6. The saturated asphalt specimens are then placed into the pressure vessel, the vessel is sealed and the air pressure is gradually raised to 0.5 MPa.
  7. The specimens are maintained at the testing conditions, i.e. 0.5 MPa and 85°C for 24 hours.
  8. After 24 hours, the target vessel temperature is reduced to 30°C and the vessel is left for 24 hours to cool. When the pressure vessel display temperature has reduced to 30°C (after the 24 hour cooling period) the air pressure is gradually released. When the vessel has achieved atmospheric pressure, it is opened and the specimens removed. Each specimen is then surface dried and weighed in air. The percentage saturation calculated at this stage is referred to as the ‘retained saturation’ (BSI 2003a, BSI 2004b, BSI 2009).
  9. The specimens are finally brought back to 20°C and the conditioned (final) stiffness modulus determined using a NAT.
  10. The ratio of the final stiffness modulus / initial stiffness modulus can thus be calculated, and is referred to as the ‘retained stiffness modulus’.

During the test there is a continuous cycling of moisture within the pressure vessel, which causes condensation on the underside of the top lid and ‘dripping’ onto the top specimen. There is then a cascading effect where progressively smaller amounts of water ‘drip’ onto the specimens below, resulting in a decrease in retained saturation level for specimens that are located lower down inside the pressure vessel.

Ten combinations of the five aggregates (two limestones and three granites) and two bitumens (10/20 and 40/60 penetration grades) were included in the study. A standard continuously graded 0/32 mm (28 mm) dense bitumen macadam (DBM) base material was used with the five aggregate types. A target binder content of 4% by total mixture mass was selected for all the asphalt mixtures and roller compacted slabs (305 mm x 305 mm x 100 mm) were manufactured and finally cored and trimmed to produce 100 mm diameter by 60 mm high specimens with a target air voids content of between 8 and 10% (typical of field cores). Only cores that achieved this target were selected for the SATS test.



948 Figure 9. SATS results for asphalt mixtures with 10/20 pen bitumen



962 Figure 10. SATS results for asphalt mixtures with 40/60 pen bitumen

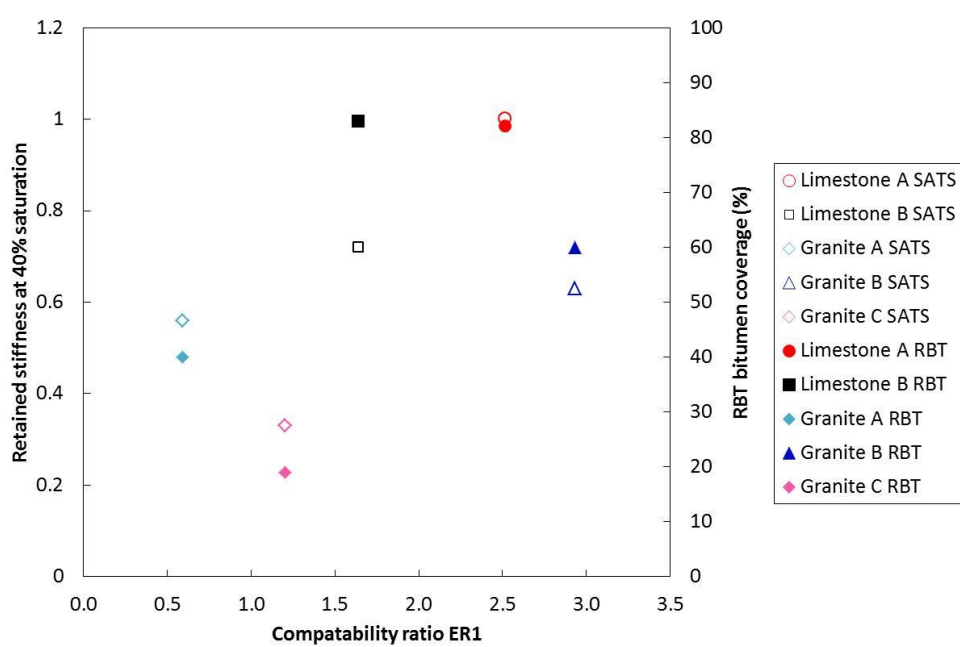
963

964 Results from the SATS tests using the 10/20 and 40/60 pen bitumen can be seen in  
 965 Figures 9 and 10. Both sets of results demonstrate the high moisture resistance of the  
 966 mixtures made with limestone aggregate. It can be seen that the retained stiffness for  
 967 the limestone mixtures is in excess of 0.6, whereas the results for Granite C mixtures  
 968 are generally in the range between 0.2 and 0.5. The results for Granite A and B  
 969 mixtures for asphalt mixtures using both the 10/20 and 40/60 pen bitumen tend to be

970 superior to those seen for Granite C. The results for the 10/20 pen bitumen (Figure 9)  
 971 even show the performance for Granite A and B to be comparable to those of the two  
 972 limestone mixtures although the saturation levels for the Granite A mixtures are  
 973 relatively low. Granite A also has a similar performance to the two limestone  
 974 aggregates for the softer 40/60 pen bitumen asphalt mixtures in Figure 10, although  
 975 once again the saturation levels are considerably lower than those experienced for the  
 976 other four mixtures.  
 977

## 978 5. Relation between intrinsic adhesion, stripping and moisture damage

980 As previously indicated, the key objective of this study was to determine if the  
 981 moisture sensitivity assessment parameters for different bitumen-aggregate  
 982 combinations obtained by using surface energy parameters of the individual materials  
 983 can identify ‘good’ and ‘poor’ performing asphalt mixtures and to determine how the  
 984 surface energy-based prediction compare with two standard types of test, for example  
 985 the RBT (stripping) and SATS (asphalt mixture) procedures. Previous studies have  
 986 shown that both the BWT and TWIT empirical tests have poor correlation with  
 987 surface energy parameters and SATS results due to the insufficient sensitivity of these  
 988 two aggregate-bitumen stripping tests (Liu et al., 2014).



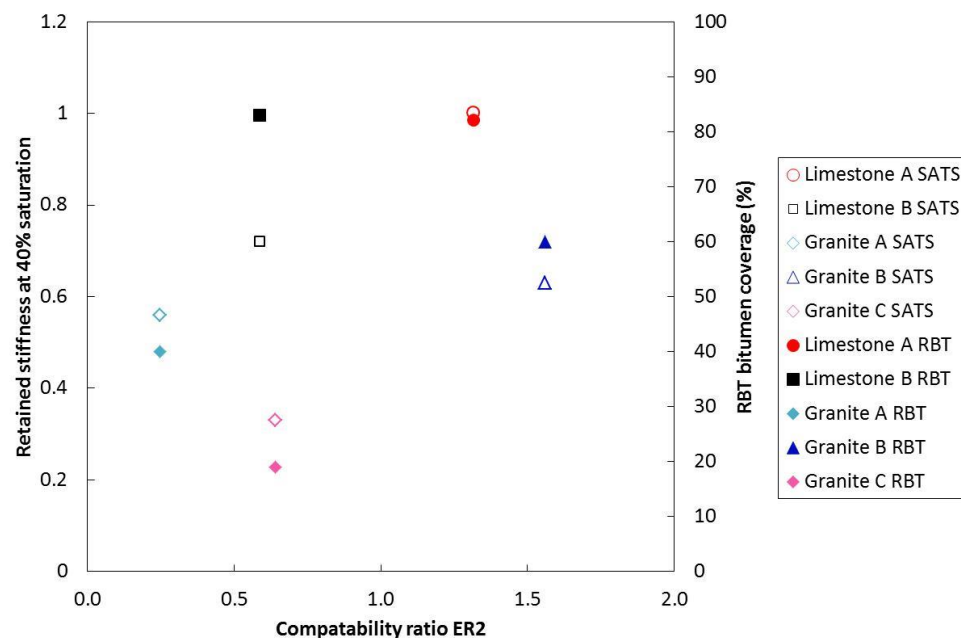
1003 Figure 11. Relationship between SATS, RBT and ER<sub>1</sub>

1004 Figures 11 to 14 show plots depicting the relationships between SATS retained  
 1005 stiffness (at 40% moisture saturation), the RBT percent bitumen coverage (after 72  
 1006 hours) and the four bond energy parameters ( $ER_1$ ,  $ER_2$ ,  $ER_3$  and  $ER_4$ ) for all mixtures  
 1007 produced with the 40/60 pen bitumen. It is worth reiterating that the energy ratios  
 1008 used in Figures 11 to 14 for Limestone B (black squares) are conservative values and  
 1009 are expected to be higher (located further to the right in the graphs) as discussed in  
 1010 Section 2.4. The SATS results at 40% moisture saturation have been determined by  
 1011 fitting a linear regression line to the data in Figure 10 and calculating the resulting  
 1012 retained stiffness at 40% moisture saturation (Grenfell et al., 2012).

1013

1014 In all cases a higher value of the parameter suggests better resistance to moisture  
 1015 damage. On this basis, aggregate-bitumen combinations plotting near the upper right  
 1016 hand side of the plot (equivalent to higher values of energy ratio, RBT coverage  
 1017 and/or SATS retained stiffness) are expected to be more moisture resistant than  
 1018 mixtures plotting in the lower left hand side. The results show in general that for all  
 1019 four plots the limestone mixtures tend to perform better than the granite mixtures with  
 1020 results in the upper right hand quadrant. The order of the two limestones does  
 1021 however change once the SSA of the two aggregates is included in the energy ratio  
 1022 ( $ER_3$  and  $ER_4$  in Figures 13 and 14) compared to  $ER_1$  and  $ER_2$  in Figures 11 and 12.

1023



1036  
 1037 Figure 12. Relationship between SATS, RBT and  $ER_2$

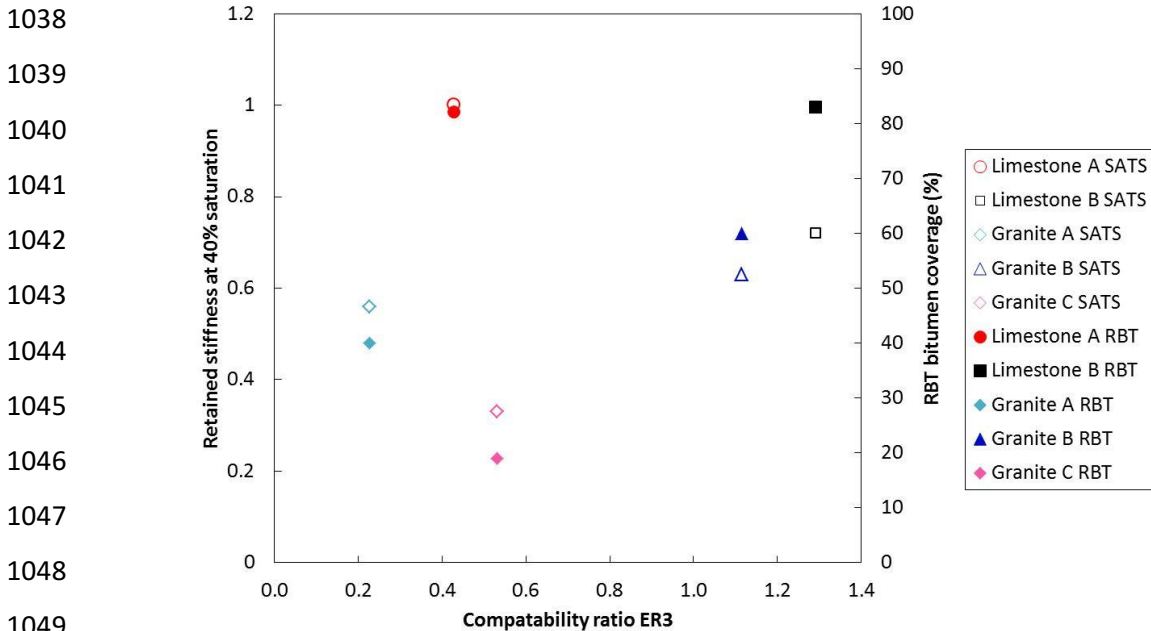


Figure 13. Relationship between SATS, RBT and  $ER_3$

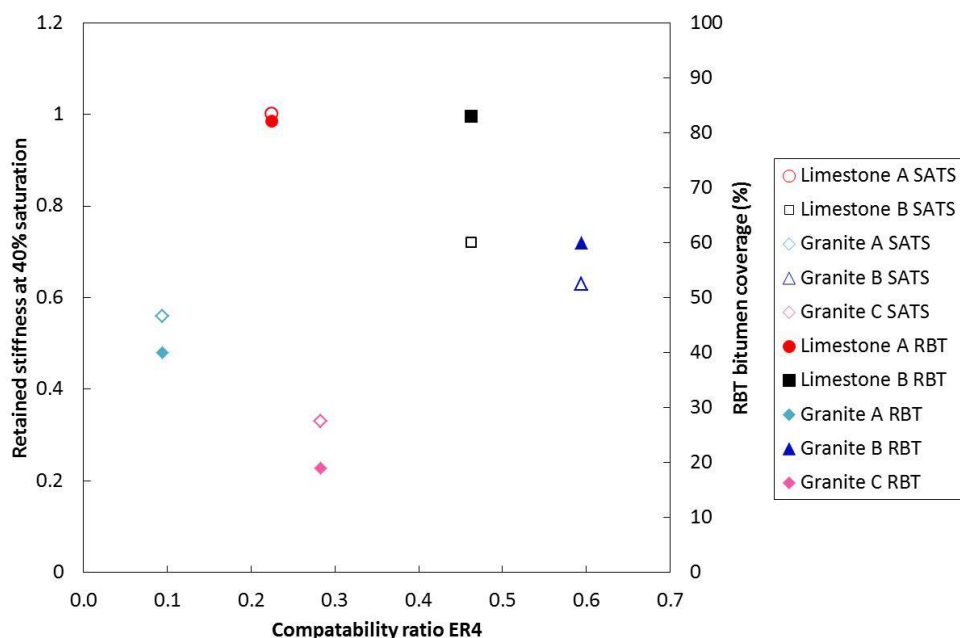


Figure 14. Relationship between SATS, RBT and  $ER_4$

In terms of the three granite aggregates, there is a fair degree of scatter with Granite A tending to have the lowest values (low predicted moisture performance) based on intrinsic adhesion and energy ratios but intermediate actual performance in terms of RBT and SATS). The results for Granite B tend to sit in the upper right hand quadrant

1072 and demonstrate comparable moisture damage performance to that seen for the two  
1073 limestone aggregate mixtures. However, the results for Granite C tend to consistently  
1074 fall in the lower left hand quadrant.

1075

1076 The ‘good’ performance of most of the limestone mixtures observed in this study can  
1077 be attributed to their physico-chemical and mineralogical characteristics, while the  
1078 range of performance found for the granite aggregates reflects the mineralogical  
1079 complexity of these aggregate types.

1080

## 1081 **6. Conclusions**

1082

1083 This paper presents results from stripping tests, such as the RBT, and asphalt mixture  
1084 moisture conditioning procedures, such as SATS, in an attempt to better understand  
1085 the underlying processes and mechanisms of moisture damage with the help of  
1086 surface energy measurements on the constituent materials (bitumen and aggregates)  
1087 and aggregate mineralogy from MLA measurements. The following conclusions were  
1088 reached based on the results presented in the paper.

1089

- 1090 • Surface energy parameters obtained from the DCA testing suggests cohesive  
1091 strength varies with bitumen grade. Surface energy of the soft bitumen (70/100  
1092 pen) was approximately 60% that of the stiffer bitumens (10/20 and 40/60  
1093 pen).
- 1094 • The adhesive bond strengths for both the dry and the wet conditions were used  
1095 to compute four compatibility ratios using the surface energy parameters  
1096 obtained for the bitumen and aggregates. Higher magnitudes of the ratios  
1097 suggest better resistance to moisture damage. The results show that for a given  
1098 aggregate, moisture resistance of stiffer binders is higher than softer binders.  
1099 The results also show that for a given bitumen grade, and for the aggregates  
1100 considered in this study, the limestone aggregate mixtures should exhibit  
1101 higher resistance (higher ratios) to moisture damage.
- 1102 • The four aggregate-bitumen bond energy parameters ( $ER_1$ ,  $ER_2$ ,  $ER_3$  and  $ER_4$ )  
1103 can be used to predict moisture sensitivity of asphalt mixtures using threshold  
1104 values (0.75 for  $ER_1$ , 0.50 for  $ER_2$ , 0.50 for  $ER_3$  and 0.35 for  $ER_4$ ) defined to  
1105 separate ‘good’ from ‘poor’ moisture damage performing aggregate-bitumen

combinations. Most of the aggregates that were identified as ‘poor’ aggregates in this study have also been found to perform poorly in previous studies. In general Limestone A and B can be defined as ‘good’ while Granite C can be defined as ‘poor’. The remaining two granite aggregates (Granite A and B) can be considered to have intermediate moisture damage performance.

- The bond energy parameters ( $ER_1$ ,  $ER_2$ ,  $ER_3$  and  $ER_4$ ) have been developed for aggregate-binder systems that demonstrate a negative value for the work of adhesion under ‘wet’ conditions ( $W_{BWA}^a$ ) and are therefore are not applicable for the systems containing Limestone B which produced positive values of  $W_{BWA}^a$ . It is therefore important to consider the energy ratio results for Limestone B as conservative values.
- Compared to the  $ER_1$  and  $ER_2$  parameters, the results for  $ER_3$  and  $ER_4$  showed the significant influence of SSA on the selection of ‘good’ versus ‘poor’ moisture damage performing aggregate-bitumen combinations. Because of the apparent large influence of SSA on moisture sensitivity of asphalt mixtures shown in this study, the bond parameters  $ER_3$  and  $ER_4$  appear to be more suitable indices for determining the performance of the different aggregate-bitumen combinations with a clear distinction in terms of ‘good’ and ‘poor’ aggregates.
- Results from the RBT showed that the percentage of bitumen coverage (a measure of adhesiveness) varies depending on aggregate type. About 90% of the limestone aggregates remained coated with bitumen at the end of the rolling bottle test compared with only 20% for one of the granite aggregate. This suggests that in the presence of moisture, limestone aggregates will generally tend to maintain a better adhesive bond with bitumen than granite aggregates although this will depend on the specific mineralogy of the granite.
- Moisture damage factors (moisture factors) obtained from the SATS tests for limestone aggregate asphalt mixtures were comparatively higher than that for certain granite mixtures. Higher moisture factors indicate better moisture resistance.
- Mineralogical testing of the aggregates, using MLA, showed considerable differences not only between limestone and granite but also between different granites. Differences in moisture sensitivity of the mixtures observed in this

1139 study for the different aggregates can be attributed in part to aggregate  
1140 mineralogy.

- 1141 • It is concluded that moisture resistance of asphalt mixtures are influenced by  
1142 the mineralogical composition of the aggregates as well as the adhesive bond  
1143 between the aggregate and bitumen in the presence of moisture. Both the RBT  
1144 and SATS are useful in evaluating moisture damage in asphalt mixtures as the  
1145 ranking obtained in these empirical tests are similar to surface energy and  
1146 mineralogical characteristics of the asphalt mixtures.
- 1147 • The surface energy testing protocols and adhesive bond strength calculations  
1148 can be used to compliment available asphalt mixture design methods by  
1149 identifying compatible bitumen-aggregate combinations. Surface energy  
1150 properties of the materials combined with the parameters obtained by  
1151 conventional moisture sensitivity assessment techniques can also contribute  
1152 towards the development of a material screening protocol. This protocol can  
1153 then be used for determining the best combinations of bitumen and aggregates  
1154 for the local road material providing better bitumen-aggregate adhesion and  
1155 less susceptibility to moisture damage/stripping.

1156

## 1157 **References**

- 1158
- 1159 Abo-Qudais S, Al-Shweily H. Effect of aggregate properties on asphalt mixtures  
1160 stripping and creep behaviour. *Constr Build Mater* 2007;21: 1886–98.
- 1161 Ahmad, N. Asphalt Mixture Moisture Sensitivity Evaluation Using Surface Energy  
1162 Parameters. *PhD Dissertation*. University of Nottingham, Nottingham, 2011.
- 1163 Airey, G.D., Masad, E.A., Bhasin, A., Caro, S. and Little, D.N. (2007) Asphalt  
1164 Mixture Moisture Damage Assessment Combined with Surface Energy  
1165 Characterization. *Proceedings of the International Conference on Advanced  
1166 Characterisation of Pavement and Soil Engineering Materials*, Vol. 1, 739-  
1167 748, Athens.
- 1168 Airey, G.D., and Choi, Y.K., (2002) State of the Art Report on Moisture Sensitivity  
1169 Test Methods for Bituminous Pavement Materials. *Road Materials and  
1170 Pavement Design*. Vol. 3, No. 4, 355-372.

- 1171 Airey, G.D., Choi, Y., Collop, A.C., Moore, A.J.V. and Elliott, R.C., (2005)  
1172 Combined laboratory ageing / moisture sensitivity assessment of high modulus  
1173 base asphalt mixtures. *Proceedings of the Association of Asphalt Paving*  
1174 *Technologists*, Vol. 74, 307-346.
- 1175 Airey, G.D., Choi, Y., Collop, A.C. and Elliott, R.C., (2003) Development of an  
1176 accelerated durability assessment procedure for high modulus base (HMB)  
1177 materials. *6th International RILEM Symposium on Performance Testing and*  
1178 *Evaluation of Bituminous Materials*, PTEBM'03, Zurich, Switzerland.
- 1179 Airey, G.D., Collop, A.C., Zoorob, S.E. and Elliott, R.C., (2008) The influence of  
1180 aggregate, filler and bitumen on asphalt mixture moisture damage.  
1181 *Construction and Building Materials*. Vol. 22, 2015–2024.
- 1182 Annual Local Authority Road Maintenance (Alarm) Survey, Asphalt Industry  
1183 Alliance, (2010). [www.asphaltindustryalliance.com/alarm.asp](http://www.asphaltindustryalliance.com/alarm.asp).
- 1184 Anon, (2000) Resistance of compacted bituminous mixtures to moisture induced  
1185 damage. AASHTO T283-99, American Association of State Highways and  
1186 Transportation Officials, USA.
- 1187 Audit Scotland, Maintaining Scotland's roads: a follow-up report, (2010). [www.audit-scotland.gov.uk/docs/central/2010/nr\\_110216\\_road\\_maintenance.pdf](http://www.audit-scotland.gov.uk/docs/central/2010/nr_110216_road_maintenance.pdf).
- 1188 Bhasin, A. (2006) Development of Methods to Quantify Bitumen-Aggregate  
1189 Adhesion and Loss of Adhesion due to Water: PhD dissertation, Texas A&M  
1190 University, USA.
- 1191 Bhasin, A., Masad, E., Little, D., and Lytton, R., (2006) Limits on Adhesive Bond  
1192 Energy for Improved Resistance of Hot-Mix Asphalt to Moisture Damage.  
1193 *Transportation research record: Journal of the Transportation Research*  
1194 *Board*, No. 1970, Washington D.C., 3-13.
- 1195 British Standards Institution, 2003a. Bituminous mixtures – Test methods for hot mix  
1196 asphalt – Part 6: Determination of bulk density of bituminous specimens, BS  
1197 EN 12697-6: London.
- 1198 British Standards Institution, 2003b. Bituminous mixtures – Test methods for hot mix  
1199 asphalt – Part 8: Determination of void characteristics of bituminous  
1200 specimens, BS EN 12697-8: London.
- 1201 British Standards Institution, 2004a. Bituminous mixtures – Test methods for hot mix  
1202 asphalt – Part 26: Stiffness, BS EN 12697-26: London.

- 1204 British Standards Institution, 2009. Bituminous mixtures – Test methods for hot mix  
1205 asphalt – Part 5: Determination of the maximum density, BS EN 12697-5:  
1206 London.
- 1207 Caro S, Masad E, Bhasin A, Little DN. Moisture susceptibility of asphalt mixtures,  
1208 Part 1: mechanisms. *Int J Pavement Eng* 2008;9:81–98.
- 1209 Caro S, Masad E, Bhasin A, Little DN. Moisture susceptibility of asphalt mixtures,  
1210 Part 2: characterisation and modelling. *Int J Pavement Eng* 2008;9:99–114.
- 1211 Caro S, Masad E, Bhasin AH, Little D. Micromechanical modelling of the influence  
1212 of material properties on moisture-induced damage in asphalt mixtures. *Constr  
1213 Build Mater* 2010;24:1174–92.
- 1214 Cheng, D. (2002) Surface Free Energy of Asphalt Aggregate System and Performance  
1215 Analysis of Asphalt Concrete based on Surface Free Energy: PhD dissertation,  
1216 Texas A&M University, USA.
- 1217 Cheng, D., Little, D.N., Lytton, R.L. and Holste, J.C. (2002a). Surface Energy  
1218 Measurement of Asphalt and Its Application to Predicting Fatigue and Healing  
1219 in Asphalt Mixtures. *Transportation Research Record: Journal of the  
1220 Transportation Research Board*, No. 1810, TRB, National Research Council,  
1221 Washington, D.C., 44-53.
- 1222 Cheng, D., Little, D.N., Lytton, R.L., and Holste, J.C., (2002b) Moisture Damage  
1223 Evaluation of Asphalt Mixtures by Considering both Moisture Diffusion and  
1224 Repeated-Load Conditions. *Transportation Research Record: Journal of the  
1225 Transportation Research Board*. TRR 1832, 42-49.
- 1226 Choi, Y.K., Collop, A.C., Airey, G.D., Elliott, R.C., Williams, J. and Heslop, M.W.,  
1227 (2002) Assessment of the durability of high modulus base (HMB) materials.  
1228 *6th International Conference on the Bearing Capacity of Roads, Railways and  
1229 Airfields*, Lisbon, Portugal.
- 1230 Choi, Y.C., (2005) Development of the saturation Ageing Tensile Stiffness (SATS)  
1231 Test for High Modulus Base Materials. PhD Thesis, School of Civil  
1232 Engineering, University of Nottingham, UK.
- 1233 Collop, A.C., Choi, Y.K., Airey, G.D. and Elliott, R.C., (2004a) Development of the  
1234 saturation ageing tensile stiffness (SATS) test. *Proceedings of the ICE  
1235 Transport*, 157, 163-171.

- 1236 Collop, A.C., Choi, Y.K. and Airey, G.D., (2004b) Development of a combined  
1237 ageing / moisture sensitivity laboratory test. *Euroasphalt and Eurobitume*  
1238 Congress, Vienna, Austria.
- 1239 Cooper, K.E. and Brown, S.F., 1989. Developments of a Simple Apparatus for the  
1240 Measurement of the Mechanical Properties of Asphalt Mixes. *Proceedings of*  
1241 *the Eurobitume Symposium*, Madrid, 494-498.
- 1242 Emery, J. and Seddik, H. (1997) Moisture-damage of Asphalt Pavements and  
1243 Antistripping Additives: Causes, Identification, Testing and Mitigation.  
1244 *Transportation Association of Canada*, Ottawa, Canada.
- 1245 Erbil, H.Y., (2006) Surface Chemistry of Solid and Liquid Interfaces, Blackwell  
1246 Publishing Ltd.
- 1247 Fowkes, F.M. (1962) Determination of Interfacial Tensions, Contact Angles, and  
1248 Dispersion Forces in Surfaces by Assuming Additivity of Intermolecular  
1249 Interactions in Surfaces, *Journal of Physical Chemistry*, Vol. 66, 382-382.
- 1250 Gilmore DW, Darland Jr JB, Girdler LM, Wilson DW, Scherocaman JA. Changes in  
1251 asphalt concrete durability resulting from exposure to multiple cycles of  
1252 freezing and thawing. *ASTM Spec Tech Publ* 1985;899:73–88.
- 1253 Good, R.J. and C.J. van Oss. (1991) The Modern Theory of Contact Angles and the  
1254 Hydrogen Bond Components of Surface Energies, Modern Approach to  
1255 Wettability: Theory and Application. Plenum Press, New York.
- 1256 Good, R.J. (1992) Contact Angle, Wetting, and Adhesion: A Critical Review, *Journal*  
1257 *of Adhesion Science and Technology*, Vol. 6, 1269-1302.
- 1258 Grenfell, J., Ahmad, N. Airey, G., Collop, A. and Elliott, R. (2012) Optimising the  
1259 moisture durability SATS conditioning parameters for universal asphalt  
1260 mixture application, *International Journal of Pavement Engineering*. Vol. 13,  
1261 No. 5, 433-450.
- 1262 Grenfell, J.R.A., Ahmad, N., Liu, Y., Apeagyei, A.K., Large, D. and Airey, G.D.  
1263 ‘Assessing asphalt mixture moisture susceptibility through intrinsic adhesion,  
1264 bitumen stripping and mechanical damage.’ *International Journal of Road*  
1265 *Materials and Pavement Design*, Vol. 15, No. 1, pp 131-152, 2014.
- 1266 Hognies, M., Darque-Ceretti, E., Fezai, H. and Felder, E. (2011) Influence of the  
1267 interfacial composition on the adhesion between aggregates and bitumen:  
1268 Investigations by EDX, XPS and peel tests, *International Journal of Adhesion*  
1269 *and Adhesives*. Vol. 31, Issue 5, 238-247.

- 1270 Huang S, Robertson RE, Branthaver JF, Petersen JC. Impact of lime modifica-  
1271 tion of asphalt and freeze-thaw cycling on the asphalt-aggregate interaction and  
1272 moisture resistance to moisture damage. *J Mater Civ Eng* 2005;17:711–8.
- 1273 Kandhal, P.S. (1994) Field and Laboratory Evaluation of Stripping in Asphalt  
1274 Pavements: State of the art. *Transportation Research Record: Journal of the*  
1275 *Transportation Research Board*. TRR 1454, TRB, Washington, D.C., 36-47.
- 1276 Kennedy TW, Roberts FL, Lee KW. Evaluation of moisture susceptibility of asphalt  
1277 mixtures using the texas freeze-thaw pedestal test. *Proc Assoc Asphalt*  
1278 *Pavement Technol* 1982;51:327–41.
- 1279 Kennedy TW, Roberts FL, Lee KW. Evaluation of moisture effects on asphalt  
1280 concrete mixtures. *Transp Res Rec* 1983;911:134–43.
- 1281 Kennedy TW, Roberts FL, Lee KW. Evaluating moisture susceptibility of asphalt  
1282 mixtures using the texas boiling test. *Transp Res Rec* 1984;968: 45–54.
- 1283 Kutay ME, Aydilek AH, Masad E. Computational and experimental evaluation of  
1284 hydraulic conductivity anisotropy in hot-mix asphalt. *Int J Pavement Eng*  
1285 2007;8:29–43.
- 1286 Little, D.N. and Bhasin, A., 2006. Using surface energy measurements to select  
1287 materials for asphalt pavement. NCHRP project 9-37, final report.  
1288 Washington, DC: Transportation Research Board, National Research Council.
- 1289 Liu, Y., Apeagyei, A.K., Ahmad, N., Grenfell, J.R.A. and Airey, G.D. ‘Examination  
1290 of moisture sensitivity of aggregate-bitumen bonding strength using loose  
1291 asphalt mixture and physico-chemical surface energy property tests.’  
1292 *International Journal of Pavement Engineering*, Vol. 15, No. 7, pp 657-670,  
1293 2014.
- 1294 Manual Series No. 24 (MS-24), (2007) Moisture Sensitivity: Best Practices to  
1295 Minimize Moisture Sensitivity in Asphalt Mixtures, Asphalt Institute, USA.
- 1296 Masad E, Al-Omari A, Chen HC. Computations of permeability tensor coefficients  
1297 and anisotropy of hot mix asphalt based on microstructure simulation of fluid  
1298 flow. *Comput Mater Sci* 2007;40:449–59.
- 1299 MCHW, 2004. Method for the Assessment of Durability of Compacted Asphalt  
1300 Mixtures using the Saturation Ageing Tensile Stiffness (SATS) Tests. Manual  
1301 of Contract Document for Highways Works: Clause 953, Highways Agency,  
1302 UK.

- 1303 Miller, J.S. and Bellinger, W.Y. (2003) Distress Identification Manual for the Long-  
1304 Term Pavement Performance Program. Publication FHWA-RD-03-031.  
1305 FHWA, Office of Infrastructure Research and Development, McLean,  
1306 Virginia.
- 1307 Petersen JC, Plancher H, Ensley EK, Venables RL, Miyake G. Chemistry of asphalt-  
1308 aggregate interaction: relationship with pavement moisture-damage prediction  
1309 test. *Transp Res Rec* 1982;843:95–104.
- 1310 Shakiba M, Abu Al-Rub RK, Darabi MK, You T, Masad EA, Little DN. Continuum  
1311 coupled moisture-mechanical damage model for asphalt concrete. *Transp Res*  
1312 *Rec* 2013;2372:72–82.
- 1313 Shaw, D. J., (1991) Introduction to Colloid and Surface Chemistry, 4th ed. Oxford.  
1314 Butterworth-Heinemann.
- 1315 Sing, K. S. W., (1969) Utilisation of Adsorption Data in the BET Region.  
1316 *Proceedings; International Symposium on Surface area Determination*,  
1317 Bristol, UK.
- 1318 Solaimanian, M., J. Harvey, M. Tahmoressi, and V. Tandon. (2003) Test Methods to  
1319 Predict Moisture Sensitivity of Hot Mix Asphalt Pavements. *Proceedings*  
1320 *National Seminar on Moisture Sensitivity of Asphalt Pavements*, San Diego,  
1321 California.
- 1322 Terrel R.L. and Al-Swailmi S. (1994) Water Sensitivity of Asphalt-Aggregate Mixes:  
1323 Test Selection. SHRP-A-403, Strategic Highway Research Program, National  
1324 Research Council, Washington, D.C.
- 1325 Vuorinen, M. and Hartikainen, O.-K., 2001. A new ultrasonic method for measuring  
1326 stripping resistance of bitumen on aggregate. *Road Materials and Pavement*  
1327 *Design*, 2 (3), 297–309
- 1328
- 1329